Eur. Phys. J. C (2017) 77:422
DOI 10.1140/epjc/s10052-017-4948-9

THE EUROPEAN PHYSICAL JOURNAL C

Regular Article - Theoretical Physics

Radiative seesaw-type mechanism of fermion masses and non-trivial quark mixing

Carolina Arbeláez[a], **A. E. Cárcamo Hernández**[b], **Sergey Kovalenko**[c], **Ivan Schmidt**[d]

Centro Científico-Tecnológico de Valparaíso-CCTVal, Universidad Técnica Federico Santa María, Casilla 110-V, Valparaiso, Chile

Received: 11 January 2017 / Accepted: 28 May 2017 / Published online: 23 June 2017

Abstract We propose a predictive inert two-Higgs doublet model, where the standard model (SM) symmetry is extended by $S_3 \otimes Z_2 \otimes Z_{12}$ and the field content is enlarged by extra scalar fields, charged exotic fermions and two heavy right-handed Majorana neutrinos. The charged exotic fermions generate a non-trivial quark mixing and provide one-loop-level masses for the first- and second-generation charged fermions. The masses of the light active neutrinos are generated from a one-loop-level radiative seesaw mechanism. Our model successfully explains the observed SM fermion mass and mixing pattern.

1 Introduction

Despite its great success, the standard model (SM) does not address several fundamental issues such as, for example, the number of fermion families and the observed pattern of fermion masses and mixing. As is well known, in the quark sector the mixing is small while in the lepton sector two of the mixing angles are large. The three neutrino flavors mix with each other and at least two of the neutrinos have non-vanishing masses, which according to neutrino oscillation experimental data must be smaller than the SM charged fermion masses by many orders of magnitude. This so called "flavor puzzle" motivates extensions of the SM with larger scalar and/or fermion sector and with extended gauge groups, supplemented with discrete flavor symmetries, so that the resulting fermion mass matrix textures would explain the observed pattern of fermion masses and mixing. The implementation of these discrete flavor symmetries in several extensions of the SM is expected to provide an elegant solution of the "flavor puzzle" (for recent reviews on discrete flavor groups see, for instance, Refs. [1–4]). In fact, considerable attention has already been paid in the literature to the S_3 [5–25] A_4 [26–54], S_4 [55–63], T_7 [64–72] and $\Delta(27)$ [73–91] flavor groups. Several models with discrete flavor symmetries, which bring about radiative seesaw mechanisms of fermion mass generation, have also been discussed in the literature [92–99]. A typical flaw of these models is the large number of free parameters and consequent limited predictive power, since they lack a mechanism underlying the observed hierarchy of quark mixing angles and masses. The experimental data suggest an empirical relation of the Cabbibo mixing angle to the first- and second-generation down-type quark masses $\sin\theta_C \sim \sqrt{\frac{m_d}{m_s}}$ [100–102], which seems to imply a radiative seesaw mechanism of fermion mass generation, where the Cabbibo mixing arises from the down-type quark sector, whereas the up quark sector contributes to the remaining mixing angles. Inspired with this observation we propose an extension of the inert two Higgs doublet model (2HDM) realizing this idea. In our model a mismatch between the down- and up-type quark mass matrix textures is introduced, by distinguishing the two Higgs doublets with respect to the Z_2 flavor symmetry, preserved at all scales. One of these doublets—the SM Higgs—is Z_2-even, while another one is Z_2-odd. In order to maintain the Z_2 symmetry intact, we assume the latter to be VEV-less. The described setup is similar to the well-known inert 2HDM [103], but with the difference that here some of the SM fermions are Z_2-odd. Furthermore, compared to Ref. [103], the discrete symmetry in our model is extended from Z_2 to $S_3 \otimes Z_2 \otimes Z_{12}$, and the field content is enlarged by extra scalars, heavy charged exotic fermions and two heavy right-handed Majorana neutrinos. Note that only the Z_2 is preserved at low energies, whereas the $S_3 \otimes Z_{12}$ symmetry is spontaneously broken. The latter allows us to explain the observed SM fermion mass and mixing pattern. In our modified inert 2HDM, the SM fermion mass and mixing pattern is due to a combina-

[a] e-mail: carolina.arbelaez@usm.cl
[b] e-mail: antonio.carcamo@usm.cl
[c] e-mail: sergey.kovalenko@usm.cl
[d] e-mail: ivan.schmidt@usm.cl

tion of tree and one-loop-level effects. At tree level only the third-generation charged fermions acquire masses and there is no quark mixing, while the first- and second-generation charged fermion masses and the quark mixing arise from one-loop-level radiative seesaw-type mechanism, triggered by virtual Z_2-charged scalar fields and electrically charged exotic fermions running inside the loops. Light active neutrino masses are generated from a one-loop-level radiative seesaw mechanism. Due to the preserved Z_2 symmetry, our model features natural dark matter candidates.

The following comparison of our model with similar models in the literature could be in order. Despite the similar quality of the data description, our model is more predictive than the model of Ref. [104], since the latter, focused only on the quark sector, has a total of 12 free parameters, whereas the quark sector of our model is described by 9 free effective parameters, which are adjusted to reproduce the 10 physical observables of the quark sector. The models of Refs. [21,105,106], Refs. [13,15,20,63,107], Refs. [76,108] and Ref. [109] possess in the quark sector 9, 10, 12, and 13 free parameters, respectively. For the lepton sector, our model is less predictive than in the quark sector, however, under some reasonable assumptions, the number of effective parameters in this sector can be reduced. As shown in detail in Sect. 3, our model can successfully accommodate the eight physical observables in the lepton sector, with only five effective free parameters for the case of normal neutrino mass hierarchy. With respect to the inverted neutrino mass hierarchy, more parameters are needed to successfully reproduce the masses and leptonic mixing angles.

The content of this paper goes as follows. In Sect. 2 we introduce the model setup. Section 3 deals with the derivation of fermion masses and mixings and provides our corresponding results. Our conclusions are stated in Sect. 6. Appendix A gives a brief description of the S_3 group. Appendix B shows the analytical expressions for the dimensionless parameters of the SM fermion mass matrices generated at one loop level.

2 The model

We consider a modified inert 2HDM, with the Standard Model gauge symmetry supplemented with the $S_3 \otimes Z_2 \otimes Z_{12}$ discrete group, and a scalar sector composed of 2 scalar SM doublets, i.e., ϕ_1 and ϕ_2 plus 4 scalar SM singlets. Out of these four SM scalar singlets, two scalar fields are grouped in a S_3 doublet, whereas the remaining ones are assigned to be one S_3 trivial singlet and one S_3 non-trivial singlet. The Z_2 symmetry is assumed to be preserved whereas the $S_3 \otimes Z_{12}$ discrete group is broken at certain scale $\Lambda_{\rm int}$. The fermion sector of the SM is extended to include four SM gauge singlet charged leptons E_{1L}, E_{2L}, E_{1R} and E_{2R}, two right-handed neutrinos N_{1R}, N_{2R} and four $SU(2)_L$ singlet heavy quarks T_{nL}, T_{nR}, B_{nL}, B_{nR} $(n = 1, 2)$. The reasons for these specific choices will be explained below. It is assumed that the heavy exotic T_n and B_n quarks have electric charges equal to $\frac{2}{3}$ and $-\frac{1}{3}$, respectively. The $S_3 \otimes Z_2 \otimes Z_{12}$ assignments of the scalar fields are:

$$\begin{aligned}
&\phi_1 \sim (\mathbf{1}, 1, 1)\,, \quad \phi_2 \sim (\mathbf{1}, -1, 1)\,,\\
&\xi \sim (\mathbf{2}, 1, 1)\,, \quad \eta \sim (\mathbf{1}, -1, 1)\,,\\
&\tau \sim \left(\mathbf{1}', 1, e^{-\frac{i\pi}{6}}\right).
\end{aligned} \tag{1}$$

The requirement of unbroken Z_2 symmetry implies that the Z_2 charged scalar fields ϕ_2 and η do not acquire vacuum expectation values. The remaining scalar fields, i.e., ϕ_1, ξ and τ, which are neutral under the Z_2 symmetry, have non-vanishing vacuum expectation values. Let us give a motivation for the above presented extension (1) of the scalar sector of the original inert 2HDM [103]. One Z_2 odd SM singlet scalar η (apart from the Z_2 odd scalar doublet ϕ_2) is needed to implement the radiative seesaw mechanism of fermion mass generation. It yields a non-trivial quark mixing, provides masses for the first- and second-generation charged fermions and contributes to the light active neutrino masses. Furthermore, one Z_{12}-charged SM singlet scalar (τ) is needed to generate the SM charged fermion mass and quark mixing pattern compatible with the observations. We also need an S_3-doublet scalar (ξ) to non-trivially couple it to the first- and second-generation right-handed SM down-type quarks, which we unify into an S_3-doublet.

We decompose the Higgs doublets ϕ_1 and ϕ_2 in the standard way as

$$\begin{aligned}
&\phi_l = \begin{pmatrix} \varphi_l^+ \\ \frac{1}{\sqrt{2}}\left(v_l + \mathrm{Re}\,\phi_l^0 + i\,\mathrm{Im}\,\phi_l^0\right) \end{pmatrix},\\
&v_l = v\delta_{l1}, \quad l = 1, 2.
\end{aligned} \tag{2}$$

Here v is a Higgs VEV breaking the electroweak symmetry.

The S_3 symmetry is broken by the VEV of the S_3 scalar doublet ξ. We choose the VEV alignment

$$\langle \xi \rangle = v_\xi\,(1, 0)\,, \tag{3}$$

compatible with the scalar potential minimization condition as demonstrated in Ref. [20]. In the literature there have been constructed several S_3 flavor models with the similar VEV alignment of an S_3 scalar doublet (see for instance Refs. [13,15,20,21]).

The $S_3 \otimes Z_2 \otimes Z_{12}$ assignments of the fermions of the model are as follows:

$$\begin{aligned}
&q_{1L} \sim \left(\mathbf{1}', 1, 1\right), \quad q_{2L} \sim (\mathbf{1}, 1, 1)\,, \quad q_{3L} \sim (\mathbf{1}, 1, 1)\,,\\
&u_{3R} \sim (\mathbf{1}, 1, 1)\,, \quad u_{1R} \sim \left(\mathbf{1}', -1, -1\right),\\
&u_{2R} \sim \left(\mathbf{1}, -1, e^{\frac{i\pi}{3}}\right)
\end{aligned}$$

$$
\begin{aligned}
&D_R = (d_{1R}, d_{2R}) \sim \left(\mathbf{2}, -1, e^{\frac{i\pi}{3}}\right), \quad d_{3R} \sim \left(\mathbf{1}', 1, i\right), \\
&l_{1L} \sim (\mathbf{1}, 1, 1), \quad l_{2L} \sim (\mathbf{1}, 1, 1), \quad l_{3L} \sim (\mathbf{1}, 1, 1), \\
&l_{1R} \sim (\mathbf{1}, -1, -1), \quad l_{2R} \sim \left(\mathbf{1}', -1, i\right), \\
&\quad l_{3R} \sim \left(\mathbf{1}', 1, i\right), \\
&T_{1L} \sim (\mathbf{1}, -1, 1), \quad T_{1R} \sim \left(\mathbf{1}', -1, 1\right), \\
&\quad T_{2L} \sim (\mathbf{1}, -1, 1), \quad T_{2R} \sim (\mathbf{1}, -1, 1), \\
&B_{1L} \sim (\mathbf{1}, 1, 1), \quad B_{1R} \sim \left(\mathbf{1}', -1, 1\right), \\
&\quad B_{2L} \sim \left(\mathbf{1}', 1, 1\right), \quad B_{2R} \sim (\mathbf{1}, -1, 1), \\
&E_{1L} \sim (\mathbf{1}, -1, 1), \quad E_{1R} \sim (\mathbf{1}, -1, 1), \\
&\quad E_{2L} \sim (\mathbf{1}, -1, 1), \quad E_{2R} \sim (\mathbf{1}, -1, 1), \\
&N_{1R} \sim (\mathbf{1}, -1, 1), \quad N_{2R} \sim (\mathbf{1}, -1, 1). \qquad (4)
\end{aligned}
$$

Now it is timely to comment on the reasons for the introduction of the extended symmetry $S_3 \otimes Z_2 \otimes Z_{12}$. The S_3 symmetry reduces the number of parameters in the Yukawa sector of the model, improving its predictivity. The Z_{12} symmetry shapes the hierarchical structure of the fermion mass matrices that gives rise to the observed charged fermion mass and quark mixing pattern. The preserved Z_2 symmetry selects the allowed entries in the quark mass matrices, so that the down-type quark sector contributes to the Cabbibo mixing, whereas the up-type quark sector contributes to the remaining mixing angles. The Z_2 symmetry allows also the implementation of a radiative seesaw-type mechanism (induced by the Z_2 charged scalar fields and the exotic charged fermions running in the internal lines of the loop), which gives rise to a non-trivial quark mixing and generates the masses for the first- and second-generation charged fermions. Besides that, due to the unbroken Z_2 symmetry, light active neutrino masses receive contributions from a one loop radiative seesaw mechanism (induced by the η and ϕ_2 scalar fields and the heavy Majorana neutrinos N_{1R} and N_{2R} running in the internal lines of the loops). Let us note that the masses of the light active neutrinos are generated from a one-loop-level radiative seesaw mechanism. It is worth mentioning that in order to be compatible with the neutrino oscillation data, we need at least two light massive active neutrinos. Having only one right-handed Majorana neutrino, will lead to two massless active neutrinos, which is in clear contradiction with the experimental data on neutrino oscillation experiments. That is why we introduced in the model two massive right-handed neutrinos N_{1R}, N_{2R} , which is the minimal number necessary for this purpose, both for normal and inverted neutrino mass hierarchy. For similar reasons we introduced in our model four $SU(2)_L$ singlet heavy quarks T_{nL}, T_{nR}, B_{nL}, B_{nR} $(n = 1, 2)$, necessary to avoid the appearance of massless charged SM fermions.

With the above particle content, the following quark and lepton Yukawa terms, invariant under the symmetries of the model, arise:

$$
\begin{aligned}
\mathcal{L}_Y^q = {} & m_{T_1}\overline{T}_{1L}T_{1R} + m_{T_2}\overline{T}_{2L}T_{2R} + y_3^{(u)}\overline{q}_{3L}\widetilde{\phi}_1 u_{3R} \\
& + y_1^{(u)}\overline{q}_{1L}\widetilde{\phi}_2 T_{1R} + x_1^{(u)}\overline{T}_{1L}\eta u_{3R} \\
& + y_2^{(u)}\overline{q}_{2L}\widetilde{\phi}_2 T_{2R} + x_2^{(u)}\overline{T}_{2L}\eta u_{3R} \\
& + x_3^{(u)}\overline{T}_{1L}\eta u_{1R}\frac{\tau^6}{\Lambda^6} + x_4^{(u)}\overline{T}_{2L}\eta u_{2R}\frac{\tau^2}{\Lambda^2} \\
& + m_{B_1}\overline{B}_{1L}B_{1R} + m_{B_2}\overline{B}_{2L}B_{2R} + y_3^{(d)}\overline{q}_{3L}\phi_1 d_{3R}\frac{\tau^3}{\Lambda^3} \\
& + x_2^{(d)}\overline{B}_{1L}\eta D_R\frac{\xi\tau^2}{\Lambda^3} + x_4^{(d)}\overline{B}_{2L}\eta D_R\frac{\xi\tau^2}{\Lambda^3} \\
& + y_1^{(d)}\overline{q}_{1L}\phi_2 B_{1R} + x_1^{(d)}\overline{B}_{1L}\eta D_R\frac{\xi\xi\tau^2}{\Lambda^4} \\
& + y_2^{(d)}\overline{q}_{2L}\phi_2 B_{2R} + x_3^{(d)}\overline{B}_{2L}\eta D_R\frac{\xi\xi\tau^2}{\Lambda^4} + h.c., \qquad (5)
\end{aligned}
$$

$$
\begin{aligned}
\mathcal{L}_Y^l = {} & m_{E_1}\overline{E}_{1L}E_{1R} + m_{E_2}\overline{E}_{2L}E_{2R} + y_3^{(l)}\bar{l}_{3L}\phi_1 l_{3R}\frac{\tau^3}{\Lambda^3} \\
& + x_1^{(l)}\bar{l}_{1L}\phi_2 E_{1R} + y_1^{(l)}\overline{E}_{1L}\eta l_{1R}\frac{\tau^6}{\Lambda^6} \\
& + x_2^{(l)}\bar{l}_{2L}\phi_2 E_{1R} + y_2^{(l)}\overline{E}_{1L}\eta l_{2R}\frac{\tau^3}{\Lambda^3} \\
& + x_3^{(l)}\bar{l}_{1L}\phi_2 E_{2R} + y_3^{(l)}\overline{E}_{2L}\eta l_{1R}\frac{\tau^6}{\Lambda^6} \\
& + x_4^{(l)}\bar{l}_{2L}\phi_2 E_{2R} + y_4^{(l)}\overline{E}_{2L}\eta l_{2R}\frac{\tau^3}{\Lambda^3} \\
& + y_{11}^{(\nu)}\bar{l}_{1L}\widetilde{\phi}_2 N_{1R} + y_{21}^{(\nu)}\bar{l}_{2L}\widetilde{\phi}_2 N_{1R} \\
& + y_{31}^{(\nu)}\bar{l}_{3L}\widetilde{\phi}_2 N_{1R} + y_{12}^{(\nu)}\bar{l}_{1L}\widetilde{\phi}_2 N_{2R} \\
& + y_{22}^{(\nu)}\bar{l}_{2L}\widetilde{\phi}_2 N_{2R} + y_{32}^{(\nu)}\bar{l}_{3L}\widetilde{\phi}_2 N_{2R} \\
& + m_{1N}\overline{N}_{1R}N_{1R}^c + m_{2N}\overline{N}_{2R}N_{2R}^c + h.c. \qquad (6)
\end{aligned}
$$

Here we considered $S_3 \otimes Z_2$ soft breaking mass terms for the charged exotic fermions. In addition, we have neglected the mixings between the T_1 (B_1) and T_2 (B_2) exotic quarks as well as the mixings between the E_1 and E_2 charged exotic leptons, by considering these charged exotic fermions as physical eigenstates. After the spontaneous breaking of the electroweak and $S_3 \otimes Z_{12}$ discrete symmetries, these interactions generate at tree- and one-loop-levels the quark and lepton mass matrices. The one loop Feynman diagrams contributions to the fermion mass matrices are shown in Fig. 1.

The hierarchy of charged fermion masses and quark mixing angles arises in our model from the breaking of the Z_{12} discrete group. In order to relate the quark masses with the quark mixing parameters, the VEVs of the SM scalar singlets ξ and τ are set as follows:

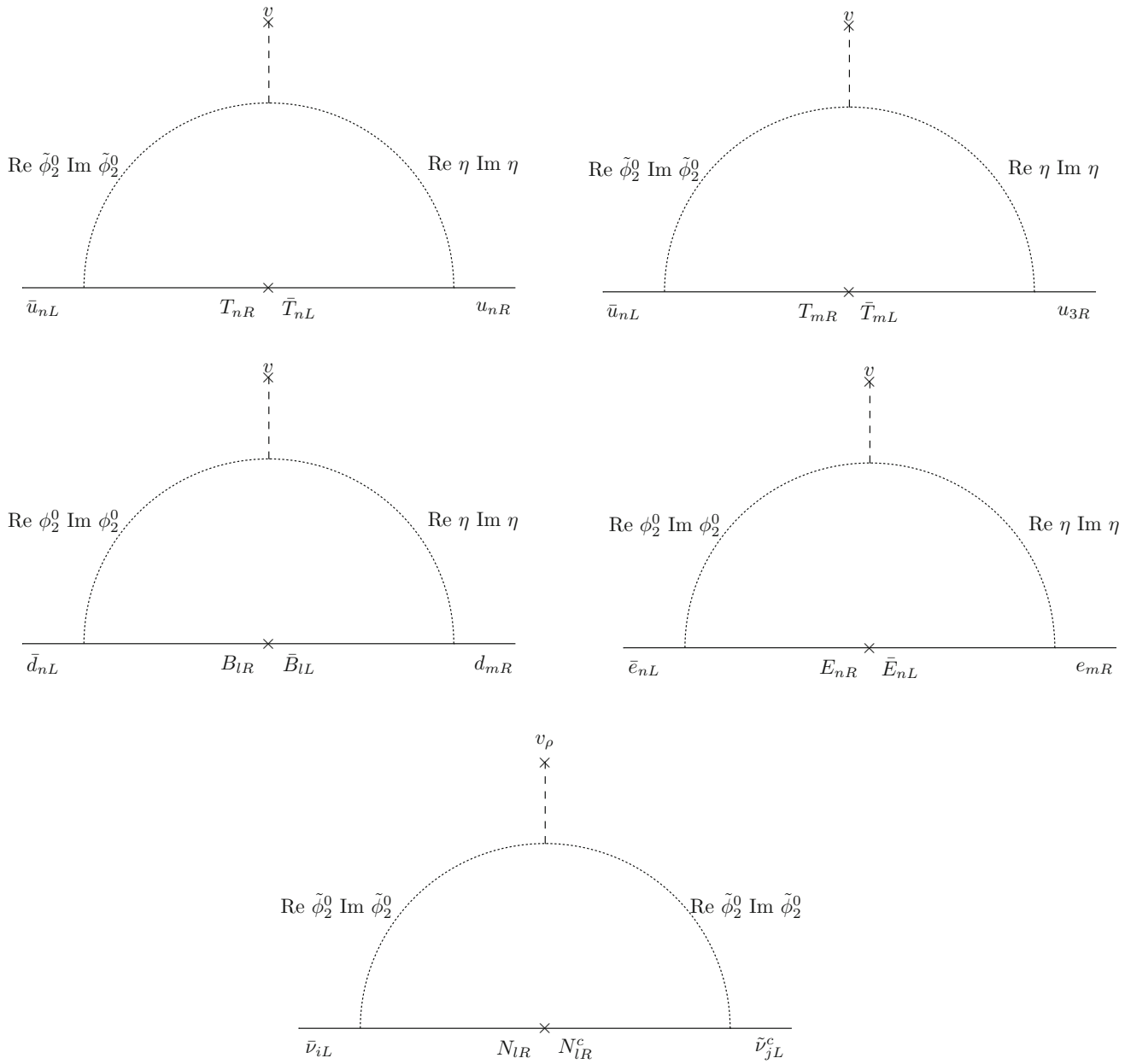

Fig. 1 One loop Feynman diagrams contributions to the fermion mass matrices. Here $n = 1, 2$, $m = 1, 2$ and $l = 1, 2$

$$v_\xi \sim \Lambda_{\text{int}} \sim v_\tau = \lambda\Lambda, \tag{7}$$

where $\lambda = 0.225$ is one of the Wolfenstein parameters and Λ corresponds to the model cutoff.

From the quark Yukawa interactions it follows that the heavy exotic T_n (B_n) quarks ($n = 1, 2$) will have a dominant decay mode into a SM up- (down-) type quark and a heavy CP even or CP odd neutral Higgs boson, which is identified as missing energy, due to the preserved Z_2 symmetry. Furthermore, from the lepton Yukawa interactions it follows that the charged exotic leptons E_n ($n = 1, 2$) will decay dominantly into a SM charged lepton and a heavy CP even or CP odd neutral Higgs boson. The exotic T_n and B_n quarks are produced in pairs at the LHC via gluon fusion and the Drell–Yan mechanism, and the charged exotic leptons E_n ($n = 1, 2$) are also produced in pairs but only via the Drell–Yan mechanism. Thus, observing an excess of events with respect to the SM background in the dijet and opposite sign dileptons final states can be a signal in support of this model at the LHC. On the other hand, it is worth mentioning that a heavy CP even Higgs can be produced at the LHC in association with a CP odd Higgs boson via Drell–Yan annihilation, with a cross section of about 0.1 fb for heavy CP even and CP odd scalar masses of 600 GeV and LHC center of

mass energy of $\sqrt{s} = 13$ TeV. To conclude this section, let us comment on the $h \to \gamma\gamma$ decay in our model, where h is the 126 GeV Higgs boson. In the standard model, this decay is dominated by W loop diagrams, which can interfere destructively with the subdominant top quark loop; whereas In the 2HDM, the $h \to \gamma\gamma$ decay receives additional contributions from loops with charged scalars $H^{\pm}$, proportional to $\sin 2\beta$ (for the case where the Higgs doublets have different Z_N charges), where $\tan\beta = v_2/v_1$ (cf. Ref. [20]). In our model $\tan\beta = 0$ since $v_2 = 0$, and thus the charged Higgs boson contribution to the 126 GeV Higgs diphoton decay is absent. From the explicit form of the $h \to \gamma\gamma$ decay rate given in [20] for the 2HDM, it is easy to see that the Higgs diphoton decay rate in our model coincides with the SM expectation, since the light and heavy CP even neutral Higgs bosons do not mix, as a result of the preserved Z_2 symmetry.

3 Quark masses and mixings

From the quark sector Yukawa terms (5) we find the quark mass matrices

$$M_U = \begin{pmatrix} \varepsilon_{11}^{(u)}\lambda^6 & 0 & \varepsilon_{13}^{(u)} \\ 0 & \varepsilon_{22}^{(u)}\lambda^2 & \varepsilon_{23}^{(u)} \\ 0 & 0 & y_3^{(u)} \end{pmatrix} \frac{v}{\sqrt{2}}, \tag{8}$$

$$M_D = \begin{pmatrix} \varepsilon_{11}^{(d)}\lambda^4 & \varepsilon_{12}^{(d)}\lambda^3 & 0 \\ \varepsilon_{21}^{(d)}\lambda^4 & \varepsilon_{22}^{(d)}\lambda^3 & 0 \\ 0 & 0 & y_3^{(d)}\lambda^3 \end{pmatrix} \frac{v}{\sqrt{2}}, \tag{9}$$

where $\varepsilon_{ij}^{(u,d)}$ are dimensionless parameters generated at one loop level whose corresponding expressions are given in Appendix B. In addition, $y_3^{(u)}$ and $y_3^{(d)}$ are $\mathcal{O}(1)$ dimensionless couplings generated at tree level from renormalizable and nonrenormalizable Yukawa terms, respectively.

In order to show that the quark textures given above can fit the experimental data, and considering that the parameters $\varepsilon_{ij}^{(u,d)}$ are generated at one loop level, we choose a benchmark scenario where we set:

$$\begin{aligned} &\varepsilon_{11}^{(u)} = a_{11}^{(u)}\lambda^2, \quad \varepsilon_{22}^{(u)} = a_{22}^{(u)}\lambda^2, \\ &\varepsilon_{13}^{(u)} = a_{13}^{(u)}\lambda^3, \quad \varepsilon_{23}^{(u)} = a_{23}^{(u)}\lambda^2, \\ &\varepsilon_{11}^{(d)} = a_{11}^{(d)}\lambda^3, \quad \varepsilon_{21}^{(d)} = a_{21}^{(d)}\lambda^2, \\ &\varepsilon_{12}^{(d)} = a_{12}^{(d)}\lambda^3, \quad \varepsilon_{22}^{(d)} = a_{22}^{(d)}\lambda^2, \end{aligned} \tag{10}$$

where $a_{nn}^{(u)}, a_{n3}^{(u)}, a_{mn}^{(d)}$ $(m, n = 1, 2)$ are $\mathcal{O}(1)$ parameters. Let us note that from the quark mass matrices given above, it follows that the Cabbibo mixing arises from the down-type quark sector, whereas the up-type quark sector contributes to the remaining mixing angles. Besides that, the low energy quark flavor data indicates that the CP violating phase in the quark sector is associated with the quark mixing angle in the 1-3 plane, as follows from the Standard parametrization of the quark mixing matrix. Consequently, in order to get quark mixing angles and a CP violating phase consistent with the experimental data, we assume that all dimensionless parameters given in Eqs. (8) and (9) are real, except $a_{13}^{(u)}$, which is taken to be complex. Since the observed pattern of charged fermion masses and quark mixing angles is generated from the $S_3 \otimes Z_{12}$ symmetry breaking, and in order to have the right value of the Cabbibo mixing, we need $a_{21}^{(d)} \approx a_{22}^{(d)}$. In addition we set $y_3^{(u)} \approx 1$, as suggested by naturalness arguments. Then the quark sector of our model contains nine effective free parameters, i.e., $a_{11}^{(u)}$, $a_{22}^{(u)}$, $|a_{13}^{(u)}|$, $a_{23}^{(u)}$, $a_{11}^{(d)}$, $a_{12}^{(d)}$, $a_{22}^{(d)}$, $y_3^{(d)}$ and the phase $\arg\left(a_{13}^{(u)}\right)$, which are fitted to reproduce the ten physical observables of the quark sector, i.e., the six quark masses, the three mixing angles and the CP violating phase. By varying these parameters, we find the quark masses, the three quark mixing angles, and the CP violating phase δ reported in Table 1, which correspond to the best-fit values:

$$\begin{aligned} &a_{23}^{(u)} \simeq 0.81, \quad |a_{13}^{(u)}| \simeq 0.3, \quad \arg\left(a_{13}^{(u)}\right) = -113^\circ, \\ &a_{22}^{(u)} \simeq 1.43, \quad a_{11}^{(u)} \simeq 1.27, \\ &a_{11}^{(d)} \simeq 0.84, \quad a_{12}^{(d)} \simeq 0.4, \quad a_{22}^{(d)} \simeq 0.57, \\ &y_3^{(d)} \simeq 1.42. \end{aligned} \tag{11}$$

Table 1 Model and experimental [110] values of the quark masses and CKM parameters

Observable	Model value	Experimental value
m_u (MeV)	1.47	$1.45^{+0.56}_{-0.45}$
m_c (MeV)	641	635 ± 86
m_t (GeV)	172.2	$172.1 \pm 0.6 \pm 0.9$
m_d (MeV)	3.00	$2.9^{+0.5}_{-0.4}$
m_s (MeV)	59.2	$57.7^{+16.8}_{-15.7}$
m_b (GeV)	2.82	$2.82^{+0.09}_{-0.04}$
$\sin\theta_{12}$	0.2257	0.2254
$\sin\theta_{23}$	0.0412	0.0413
$\sin\theta_{13}$	0.00352	0.00350
δ	68°	68°

It is worth mentioning, as follows from Eq. (B1) given in Appendix B, that the functions $\varepsilon_{11}^{(u)}, \varepsilon_{22}^{(u)}, \varepsilon_{13}^{(u)}$ and $\varepsilon_{23}^{(u)}$ depend on the dimensionless parameters $x_1^{(u)}, x_2^{(u)}, x_3^{(u)}, x_4^{(u)}, y_1^{(u)}, y_2^{(u)}$, on the masses $m_{T_1}, m_{T_2}, m_{\mathrm{Re}\,\phi_2^0}, m_{\mathrm{Re}\,\eta}, m_{\mathrm{Im}\,\phi_2^0}$ and $m_{\mathrm{Im}\,\eta}$ as well as on the trilinear scalar coupling $C_{\phi_2\phi_1\eta}$. Furthermore, the functions $\varepsilon_{11}^{(d)}, \varepsilon_{22}^{(d)}, \varepsilon_{12}^{(d)}$ and $\varepsilon_{21}^{(d)}$ depend on the dimensionless parameters $x_1^{(d)}, x_2^{(d)}, x_3^{(d)}, x_4^{(d)}, y_1^{(d)}, y_2^{(d)}$, on the masses $m_{B_1}, m_{B_2}, m_{\mathrm{Re}\,\phi_2^0}, m_{\mathrm{Re}\,\eta}, m_{\mathrm{Im}\,\phi_2^0}$ and $m_{\mathrm{Im}\,\eta}$

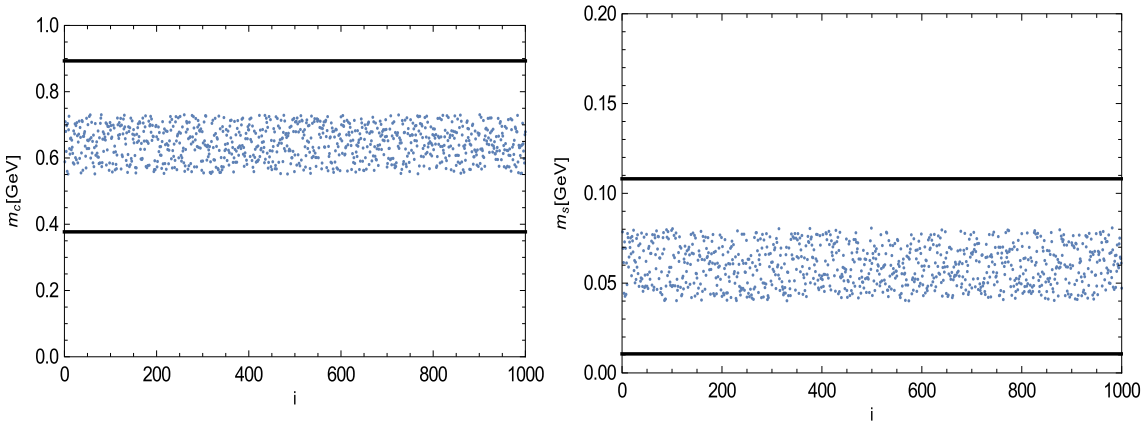

Fig. 2 Charm and strange quark masses randomly generated. The *horizonal lines* are the minimum and maximum values of the SM quark masses inside the 3σ experimentally allowed range

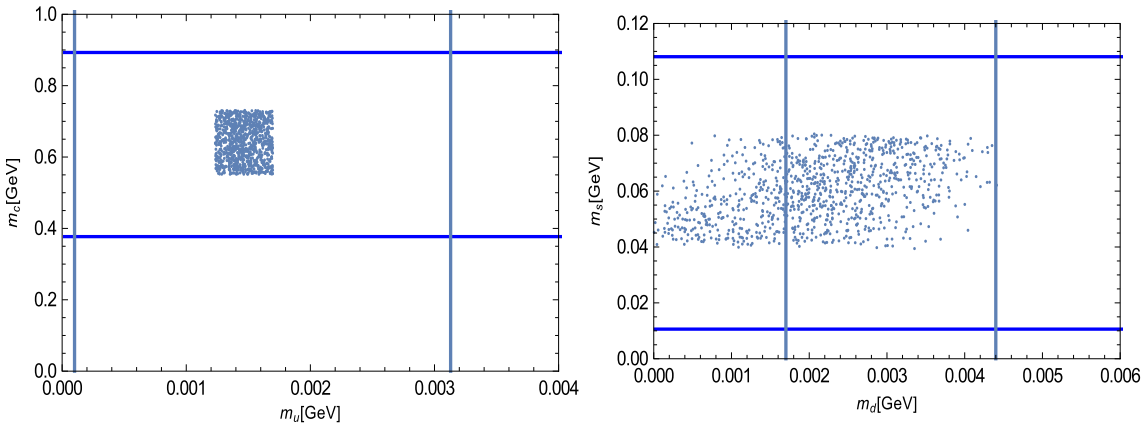

Fig. 3 Correlations between the first- and second-generation SM quark masses. The *horizonal* and *vertical lines* are the minimum and maximum values of the second- and first-generation quark masses, respectively, inside the 3σ experimentally allowed range

as well as on the trilinear scalar coupling $C_{\phi_2\phi_1\eta}$. Consequently, there is a good amount of parametric freedom to reproduce the obtained values for the $\varepsilon_{ij}^{(u,d)}$ $(i, j = 1, 2, 3)$ functions that successfully reproduce the physical observables of the quark sector. For instance, the best-fit values given above imply that $\varepsilon_{11}^{(u)} \simeq 6.4 \times 10^{-2}$, which can be obtained by setting $m_{T_1} = 1$ TeV, $m_{\mathrm{Re}\,\phi_2^0} = 420$ GeV, $m_{\mathrm{Re}\,\eta} = 560$ GeV, $m_{\mathrm{Im}\,\phi_2^0} = 600$ GeV, $m_{\mathrm{Im}\,\eta} = 800$ GeV, $C_{\phi_2\phi_1\eta} = 3$ TeV, $x_3^{(u)} = y_1^{(u)} = 3$. Similar considerations apply for the down-type quark and lepton sector.

In order to study the sensitivity of the obtained values for the SM quark masses under small variations around the best-fit values (maximum variation of $+0.2$, minimum of -0.2), we show in Fig. 2 the predicted charm and strange masses as functions of the iteration. We find that, for a slight deviation from the best-fit values, the obtained charm and strange masses stay inside the 3σ experimentally allowed range. We also have numerically checked that the remaining SM quark masses are kept inside the 3σ experimentally allowed limits when we perform small variations around the best-fit values, with the exception of the down and bottom quark masses. The sensitivity of the down-type quark mass under small variations around the best-fit values is due to the fact that all entries in the upper left block of the SM down-type quark mass matrix are different from zero, thus implying that there is an important region of parameter space where the determinant of the down-type quark mass matrix takes low values. With respect to the bottom quark mass, we find that most of the points are inside the 3σ experimentally allowed range. Those outside the 3σ experimentally allowed range correspond to values close to the lower and upper experimental bounds of the bottom quark mass. Consequently, our model is very predictive for the quark sector. Correlations between the first- and second-generation SM quark masses are shown in Fig. 3. The horizontal and vertical lines are the minimum and maximum values of the second- and first-generation quark masses, respectively, inside the 3σ experimentally allowed range.

4 Lepton masses and mixings

From the lepton Yukawa terms (6) we derive the neutrino mass matrices

$$M_l = \frac{v}{\sqrt{2}} \begin{pmatrix} a_{11}^{(l)}\lambda^8 & a_{12}^{(l)}\lambda^5 & 0 \\ a_{21}^{(l)}\lambda^8 & a_{22}^{(l)}\lambda^5 & 0 \\ 0 & 0 & y_3^{(l)}\lambda^3 \end{pmatrix}, \tag{16}$$

which implies that the following relation is fulfilled:

$$M_l M_l^T = \frac{v^2}{2} \begin{pmatrix} \left(a_{12}^{(l)}\right)^2\lambda^{10} + \left(a_{11}^{(l)}\right)^2\lambda^{16} & a_{12}^{(l)}a_{22}^{(l)}\lambda^{10} + a_{11}^{(l)}a_{21}^{(l)}\lambda^{16} & 0 \\ a_{12}^{(l)}a_{22}^{(l)}\lambda^{10} + a_{11}^{(l)}a_{21}^{(l)}\lambda^{16} & \left(a_{22}^{(l)}\right)^2\lambda^{10} + \left(a_{21}^{(l)}\right)^2\lambda^{16} & 0 \\ 0 & 0 & \left(y_3^{(l)}\right)^2\lambda^6 \end{pmatrix}. \tag{17}$$

$$M_l = \begin{pmatrix} \varepsilon_{11}^{(l)}\lambda^6 & \varepsilon_{12}^{(l)}\lambda^3 & 0 \\ \varepsilon_{21}^{(l)}\lambda^6 & \varepsilon_{22}^{(l)}\lambda^3 & 0 \\ 0 & 0 & y_3^{(l)}\lambda^3 \end{pmatrix} \frac{v}{\sqrt{2}}, \tag{12}$$

$$M_\nu = \begin{pmatrix} W_1^2 & W_1W_2\cos\varphi & W_1W_3\cos(\varphi-\varrho) \\ W_1W_2\cos\varphi & W_2^2 & W_2W_3\cos\varrho \\ W_1W_3\cos(\varphi-\varrho) & W_2W_3\cos\varrho & W_3^2 \end{pmatrix}, \tag{13}$$

where $\varepsilon_{nm}^{(l)}$ $(n, m = 1, 2)$ are dimensionless parameters generated at one loop level whose corresponding expressions are given in Appendix B. The parameters of the neutrino mass matrix of Eq. (13) take the form

$$\begin{aligned} &\overrightarrow{W_j} = \left(\frac{A_{j1}\sqrt{m_{N_1} f_1^{(\nu)}}}{64\pi^3\Lambda}, \frac{A_{j2}\sqrt{m_{N_2} f_2^{(\nu)}}}{64\pi^3\Lambda}\right), \quad j = 1,2,3 \\ &\cos\varphi = \frac{\overrightarrow{W_1}\cdot\overrightarrow{W_2}}{\left|\overrightarrow{W_1}\right|\left|\overrightarrow{W_2}\right|}, \quad \cos(\varphi-\varrho) = \frac{\overrightarrow{W}_1\cdot\overrightarrow{W_3}}{\left|\overrightarrow{W}_1\right|\left|\overrightarrow{W_3}\right|}, \quad W_j = \left|\overrightarrow{W_j}\right|, \\ &\cos\varrho = \frac{\overrightarrow{W_2}\cdot\overrightarrow{W_3}}{\left|\overrightarrow{W_2}\right|\left|\overrightarrow{W_3}\right|}, \quad A_{js} = y_{js}^{(\nu)}\frac{v}{\sqrt{2}} \quad s = 1,2, \\ &f_s = \frac{m_R^2}{m_R^2 - m_{N_s}^2}\ln\left(\frac{m_R^2}{m_{N_s}^2}\right) - \frac{m_I^2}{m_I^2 - m_{N_s}^2}\ln\left(\frac{m_I^2}{m_{N_s}^2}\right), \\ &m_R = m_{\mathrm{Re}\,\phi_2^0}, \quad m_I = m_{\mathrm{Im}\,\phi_2^0}. \end{aligned} \tag{14}$$

In order to show that the lepton textures given above can fit the experimental data, and considering that the parameters $\varepsilon_{ij}^{(l)}$ are generated at one loop level, we choose a benchmark scenario where we set:

$$\begin{aligned} &\varepsilon_{11}^{(l)} = a_{11}^{(l)}\lambda^2, \quad \varepsilon_{21}^{(l)} = a_{21}^{(l)}\lambda^2, \\ &\varepsilon_{12}^{(l)} = a_{12}^{(l)}\lambda^2, \quad \varepsilon_{22}^{(l)} = a_{22}^{(l)}\lambda^2, \end{aligned} \tag{15}$$

where $a_{nm}^{(l)}$ $(n, m = 1, 2, 3)$ are $\mathcal{O}(1)$ parameters.

Then it follows that the charged lepton mass matrix takes the following form:

The mass matrix $M_l M_l^T$ can be diagonalized by a rotation matrix R_l according to

$$\begin{aligned} R_l^T M_l M_l^T R_l &= \begin{pmatrix} m_e^2 & 0 & 0 \\ 0 & m_\mu^2 & 0 \\ 0 & 0 & m_\tau^2 \end{pmatrix}, \\ R_l &= \begin{pmatrix} \cos\theta_l & \sin\theta_l & 0 \\ -\sin\theta_l & \cos\theta_l & 0 \\ 0 & 0 & 1 \end{pmatrix}, \quad \tan\theta_l \simeq \frac{a_{12}^{(l)}}{a_{22}^{(l)}}, \end{aligned} \tag{18}$$

where the charged lepton masses are given by

$$m_e \simeq \lambda^8 \cdot \frac{\left|a_{12}^{(l)}a_{21}^{(l)} - a_{11}^{(l)}a_{22}^{(l)}\right|}{\sqrt{\left(a_{12}^{(l)}\right)^2 + \left(a_{22}^{(l)}\right)^2}}\frac{v}{\sqrt{2}}, \tag{19}$$

$$m_\mu \simeq \lambda^5 \cdot \sqrt{\left(a_{12}^{(l)}\right)^2 + \left(a_{22}^{(l)}\right)^2}\frac{v}{\sqrt{2}}, \tag{20}$$

$$m_\tau = \lambda^3 \cdot y_3^{(l)}\frac{v}{\sqrt{2}}. \tag{21}$$

Thus we correctly reproduce the charged lepton mass hierarchy from the symmetry structure of the model.

To simplify further the analysis, we set $\varphi = \varrho$, obtaining that the light neutrino mass matrix is given by

$$M_\nu = \begin{pmatrix} W_1^2 & \kappa W_1W_2 & W_1W_3 \\ \kappa W_1W_2 & W_2^2 & \kappa W_2W_3 \\ W_1W_3 & \kappa W_2W_3 & W_3^2 \end{pmatrix}, \quad \kappa = \cos\varphi. \tag{22}$$

Assuming that the neutrino Yukawa couplings are real, we find that for the normal (NH) and inverted (IH) mass hierarchies, the light neutrino mass matrix is diagonalized by a rotation matrix R_ν, according to

$$R_\nu^T M_\nu R_\nu = \begin{pmatrix} 0 & 0 & 0 \\ 0 & m_{\nu_2} & 0 \\ 0 & 0 & m_{\nu_3} \end{pmatrix},$$

$$R_\nu = \begin{pmatrix} -\frac{W_3}{\sqrt{W_1^2+W_3^2}} & \frac{W_1}{\sqrt{W_1^2+W_3^2}}\sin\theta_\nu & \frac{W_1}{\sqrt{W_1^2+W_3^2}}\cos\theta_\nu \\ 0 & \cos\theta_\nu & -\sin\theta_\nu \\ \frac{W_1}{\sqrt{W_1^2+W_3^2}} & \frac{W_3}{\sqrt{W_1^2+W_3^2}}\sin\theta_\nu & \frac{W_3}{\sqrt{W_1^2+W_3^2}}\cos\theta_\nu \end{pmatrix}, \quad \text{for NH}, \tag{23}$$

$$\tan\theta_\nu = -\sqrt{\frac{W_2^2 - m_{\nu_2}}{m_{\nu_3} - W_2^2}}, \tag{24}$$

$$m_{\nu_1} = 0, \quad m_{\nu_{2,3}} = \frac{W_1^2+W_2^2+W_3^2}{2} \mp \frac{\sqrt{\left(W_1^2 - W_2^2 + W_3^2\right)^2 + 4\kappa^2 W_2^2\left(W_1^2+W_3^2\right)}}{2}, \tag{25}$$

$$R_\nu^T M_\nu R_\nu = \begin{pmatrix} m_{\nu_1} & 0 & 0 \\ 0 & m_{\nu_2} & 0 \\ 0 & 0 & 0 \end{pmatrix},$$

$$R_\nu = \begin{pmatrix} \frac{W_1}{\sqrt{W_1^2+W_3^2}}\sin\theta_\nu & \frac{W_1}{\sqrt{W_1^2+W_3^2}}\cos\theta_\nu & -\frac{W_3}{\sqrt{W_1^2+W_3^2}} \\ \cos\theta_\nu & -\sin\theta_\nu & 0 \\ \frac{W_3}{\sqrt{W_1^2+W_3^2}}\sin\theta_\nu & \frac{W_3}{\sqrt{W_1^2+W_3^2}}\cos\theta_\nu & \frac{W_1}{\sqrt{W_1^2+W_3^2}} \end{pmatrix}, \quad \text{for IH} \tag{26}$$

$$\tan\theta_\nu = -\sqrt{\frac{W_2^2 - m_{\nu_1}}{m_{\nu_2} - W_2^2}} \tag{27}$$

$$m_{\nu_{1,2}} = \frac{W_1^2+W_2^2+W_3^2}{2} \mp \frac{1}{2}\sqrt{\left(W_1^2 - W_2^2 + W_3^2\right)^2 + 4\kappa^2 W_2^2\left(W_1^2+W_3^2\right)}, \quad m_{\nu_3} = 0. \tag{28}$$

With the rotation matrices in the charged lepton sector R_l, given by Eq. (18), and in the neutrino sector R_ν, given by Eqs. (23) and (26) for NH and IH, respectively, we find the PMNS mixing matrix:

$$U = R_l^T R_\nu, = \begin{cases} \begin{pmatrix} -\frac{W_3}{\sqrt{W_1^2+W_3^2}}\cos\theta_l & \frac{W_1}{\sqrt{W_1^2+W_3^2}}\cos\theta_l\sin\theta_\nu - \cos\theta_\nu\sin\theta_l & \sin\theta_l\sin\theta_\nu + \frac{W_1}{\sqrt{W_1^2+W_3^2}}\cos\theta_l\cos\theta_\nu \\ -\frac{W_3}{\sqrt{W_1^2+W_3^2}}\sin\theta_l & \cos\theta_l\cos\theta_\nu + \frac{W_1}{\sqrt{W_1^2+W_3^2}}\sin\theta_\nu\sin\theta_l & \frac{W_1}{\sqrt{W_1^2+W_3^2}}\sin\theta_l\cos\theta_\nu - \cos\theta_l\sin\theta_\nu \\ \frac{W_1}{\sqrt{W_1^2+W_3^2}} & \frac{W_3}{\sqrt{W_1^2+W_3^2}}\sin\theta_\nu & \frac{W_3}{\sqrt{W_1^2+W_3^2}}\cos\theta_\nu \end{pmatrix} & \text{for NH}, \\ \begin{pmatrix} \frac{W_1}{\sqrt{W_1^2+W_3^2}}\cos\theta_l\sin\theta_\nu - \cos\theta_\nu\sin\theta_l & \sin\theta_l\sin\theta_\nu + \frac{W_1}{\sqrt{W_1^2+W_3^2}}\cos\theta_l\cos\theta_\nu & -\frac{W_3}{\sqrt{W_1^2+W_3^2}}\cos\theta_l \\ \cos\theta_l\cos\theta_\nu + \frac{W_1}{\sqrt{W_1^2+W_3^2}}\sin\theta_l\sin\theta_\nu & \frac{W_1}{\sqrt{W_1^2+W_3^2}}\cos\theta_\nu\sin\theta_l - \cos\theta_l\sin\theta_\nu & -\frac{W_3}{\sqrt{W_1^2+W_3^2}}\sin\theta_l \\ \frac{W_3}{\sqrt{W_1^2+W_3^2}}\sin\theta_\nu & \frac{W_3}{\sqrt{W_1^2+W_3^2}}\cos\theta_\nu & \frac{W_1}{\sqrt{W_1^2+W_3^2}} \end{pmatrix} & \text{for IH}. \end{cases} \tag{29}$$

From the standard parametrization of the leptonic mixing matrix, it follows that the lepton mixing angles for NH and IH, respectively, are

$$\sin^2\theta_{12} = \frac{\left(\frac{W_1}{\sqrt{W_1^2+W_3^2}}\cos\theta_l\sin\theta_\nu - \cos\theta_\nu\sin\theta_l\right)^2}{1 - \left(\sin\theta_l\sin\theta_\nu + \frac{W_1}{\sqrt{W_1^2+W_3^2}}\cos\theta_l\cos\theta_\nu\right)^2},$$

$$\sin^2\theta_{13} = \left(\sin\theta_l\sin\theta_\nu + \frac{W_1}{\sqrt{W_1^2+W_3^2}}\cos\theta_l\cos\theta_\nu\right)^2,$$

$$\sin^2\theta_{23} = \frac{\left(\frac{W_1}{\sqrt{W_1^2+W_3^2}}\sin\theta_l\cos\theta_\nu - \cos\theta_l\sin\theta_\nu\right)^2}{1 - \left(\sin\theta_l\sin\theta_\nu + \frac{W_1}{\sqrt{W_1^2+W_3^2}}\cos\theta_l\cos\theta_\nu\right)^2} \quad \text{for NH} \tag{30}$$

$$\sin^2\theta_{12} = \frac{\left(\sin\theta_l\sin\theta_\nu + \frac{W_1}{\sqrt{W_1^2+W_3^2}}\cos\theta_l\cos\theta_\nu\right)^2}{1 - \frac{W_3^2\cos^2\theta_l}{W_1^2+W_3^2}},$$

$$\sin^2\theta_{13} = \frac{W_3^2\cos^2\theta_l}{W_1^2+W_3^2},$$

$$\sin^2\theta_{23} = \frac{\frac{W_3^2}{W_1^2+W_3^2}\sin^2\theta_l}{1 - \frac{W_3^2\cos^2\theta_l}{W_1^2+W_3^2}}, \quad \text{for IH}. \tag{31}$$

In the charged lepton sector the model has five free parameters $a_{11}^{(l)}, a_{12}^{(l)}, a_{21}^{(l)}, a_{22}^{(l)}, y_3^{(l)}$. Fitting Eqs. (19)–(21) for $m_{e,\mu,\tau}$ to the corresponding experimental values [111], we found $\mathcal{O}(1)$ solutions for these parameters. Therefore, we conclude that the model correctly predicts the charged lepton mass hierarchy according to Eqs. (19)–(21). On the other hand, it does not predict the particular values of the charged lepton masses. In fact, within the hierarchical structure incorporated in Eqs. (19)–(21), the five free $\mathcal{O}(1)$ parameters $a_{11}^{(l)}, a_{12}^{(l)}, a_{21}^{(l)}, a_{22}^{(l)}, y_3^{(l)}$ allow one to reproduce the experimental values of $m_{e,\mu,\tau}$ with arbitrary precision limited only by the experimental errors.

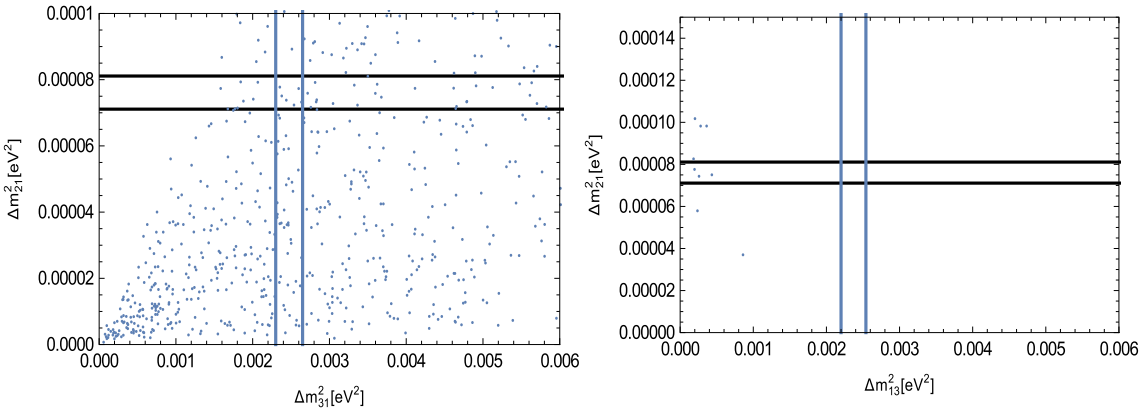

Fig. 4 Correlations between Δm^2_{21} and Δm^2_{31} for the cases of normal (*left plot*) and inverted (*right plot*) neutrino mass hierarchy. The *horizonal* and *vertical lines* are the minimum and maximum values of the neutrino mass squared splittings inside the 3σ experimentally allowed range

The charged lepton sector "contributes" to the neutrino sector with a single free parameter θ_l defined in Eq. (18). It remains unrestricted by the charged lepton masses. Thus, in the neutrino sector we have five free parameters $W_{1,2,3}, \kappa, \theta_l$ and five observables: two neutrino mass squared splittings Δm^2_{21}, Δm^2_{31} (we define $\Delta m^2_{ij} = m^2_i - m^2_j$) and three mixing angles $\sin^2\theta_{12}$, $\sin^2\theta_{13}$, $\sin^2\theta_{23}$ for both NH and IH. We solve Eqs. (25), (28) and (30), (31) with respect to the model parameters for the central values of the corresponding observables shown in Table 2. The unique solutions for NH and IH are

$$\text{for NH:}\kappa \simeq 0.7, \quad W_1 \simeq 0.09\,\text{eV}^{\frac{1}{2}},$$
$$W_2 \simeq 0.16\text{eV}^{\frac{1}{2}}, \quad W_3 \simeq 0.15\,\text{eV}^{\frac{1}{2}}, \quad \theta_l \simeq 18.95^\circ \qquad (32)$$
$$\text{for IH:}\kappa \simeq 6.11 \times 10^{-3}, \quad W_1 \simeq 0.14\,\text{eV}^{\frac{1}{2}},$$
$$W_2 \simeq 0.22\,\text{eV}^{\frac{1}{2}}, \quad W_3 \simeq 0.17\,\text{eV}^{\frac{1}{2}}, \quad \theta_l \simeq -78.30^\circ. \qquad (33)$$

Figure 4 shows the correlation between Δm^2_{21} and Δm^2_{31} for the cases of normal and inverted neutrino mass hierarchies, respectively. We find that a slight variation from the best-fit values yields, for several points of the parameter space, an important deviation in the values of the neutrino mass squared splittings and leptonic mixing parameters, especially for the case of inverted neutrino mass hierarchy.

Nevertheless the model in its present version is not predictive in the lepton sector except for the charged lepton mass hierarchy Eqs. (19)–(21). This is because the number of free parameters equals the number of observables.

However, considering the model parameters for NH in Eq. (32) we note that their numerical values $W_2 \simeq W_3, \kappa \approx 1$ may point to an approximate underlying μ–τ symmetry. In fact for $W_2 = W_3$, $\kappa = 1$ the light active neutrino mass matrix (22) coincides in structure with the μ–τ symmetric Fukuyama–Nishiura texture [114]:

$$M_\nu = \begin{pmatrix} A & B & B \\ B & C & D \\ B & D & C \end{pmatrix}. \qquad (34)$$

With this observation let us study a μ–τ symmetry inspired benchmark scenario in our model. Incorporation of the μ–τ symmetry in our model implies $W_2 = W_3$ and $\kappa = 1$ and, therefore, $C = D$ in (34) leading to two vanishing eigenvalues, which is in clear contradiction with the neutrino oscillation data. After all, this symmetry cannot be exact, since it is explicitly broken in the charged lepton sector (for more details of the phenomenological aspects of the μ–τ interchange symmetry see, for instance, Refs. [115–125]). However, the μ–τ symmetry can be incorporated in our model as a "minimally" broken symmetry. Its maximal breaking corresponds to the violation of both $W_2 = W_3$ and $\kappa = 1$ conditions. In this sense the minimal breaking is introduced by the violation of only one of these conditions. As can easily be checked the case $W_2 \neq W_3$ with $\kappa = 1$ is an inappropriate one since it has two zero eigenvalues of the neutrino mass matrix Eq. (22). Thus, we study the benchmark scenario (i) with $W_2 = W_3$ and κ being a free μ–τ symmetry breaking parameter. In this case there is only one zero neutrino mass matrix eigenvalue. Now we have four free model parameters W_1, W_2, κ and θ_l versus the five physical observables in the neutrino sector, i.e., the two neutrino mass squared splittings and the three leptonic mixing parameters. Thus, the model is able to predict one of these observables using the experimental values of the other four. Instead of doing this we conventionally fit the model parameters to the experimental values of all the five observables within the corresponding experimental errors. The best-fit results are shown in Table 2 for

$$\kappa \simeq 0.70, \quad W_1 \simeq 0.09\text{eV}^{\frac{1}{2}},$$
$$W_2 \simeq 0.16\text{eV}^{\frac{1}{2}}, \quad \theta_l \simeq 19.81^\circ, \qquad (35)$$

corresponding to the normal neutrino hierarchy. Here the parameter κ is not too far from its μ–τ symmetric value $\kappa = 1$. In the case of the inverted hierarchy it is two–three orders of magnitude away from this value and the μ–τ symmetry does not show up as an approximate symmetry of the

Table 2 The symmetry inspired benchmark scenarios (i) and (ii) versus the experimental values of the charged lepton masses [111], neutrino oscillation observables for the normal (NH) and inverted (IH) mass hierarchies [113]. Scenario (i): the four model parameters (35) fit the five neutrino oscillation observables for the NH. Scenario (ii)': from the experimental input value $m_e = 0.487$ MeV we determine a model parameter $a_{21}^{(l)} = 0.52$ and then calculate $m_\mu = 113.07$ MeV; the neutrino oscillation observables for the NH are fitted with three parameters (36). Scenario (ii)': the same as (ii), but fitting jointly the four model parameters (37) to the seven observables

Observable	Experimental value	(i)	(ii)'	(ii)
m_e (MeV)	0.487	No prediction	Input	0.43
m_μ (MeV)	102.8 ± 0.0003	No prediction	113.07	115.1
$\Delta m^2_{21}(10^{-5}\text{eV}^2)$ (NH)	$7.60^{+0.19}_{-0.18}$	7.62	7.72	7.62
$\Delta m^2_{31}(10^{-3}\text{eV}^2)$ (NH)	$2.48^{+0.05}_{-0.07}$	2.52	2.70	2.52
$\sin^2\theta_{12}$ (NH)	0.323 ± 0.016	0.324	0.258	0.303
$\sin^2\theta_{23}$ (NH)	$0.567^{+0.032}_{-0.128}$	0.542	0.526	0.527
$\sin^2\theta_{13}$ (NH)	0.0234 ± 0.0020	0.0234	0.0224	0.0204
$\Delta m^2_{21}(10^{-5}\text{eV}^2)$ (IH)	$7.60^{+0.19}_{-0.18}$	–	–	–
$\Delta m^2_{13}(10^{-3}\text{eV}^2)$ (IH)	$2.38^{+0.05}_{-0.06}$	–	–	–
$\sin^2\theta_{12}$ (IH)	0.323 ± 0.016	–	–	–
$\sin^2\theta_{23}$ (IH)	$0.573^{+0.025}_{-0.043}$	-	–	–
$\sin^2\theta_{13}$ (IH)	0.0240 ± 0.0019	–	–	–

neutrino sector. A more detailed study of this observation and its possible implementation in the model Lagrangian will be addressed elsewhere.

Let us examine even more restrictive benchmark scenario assuming additionally to $W_3 = W_2$ also the relation for the model parameters $a_{11}^{(l)} = a_{22}^{(l)} = a_{21}^{(l)} = 1$ in the sector of charged leptons e, μ. So that there is only one free parameter $a_{12}^{(l)}$ to fit m_e and m_μ using Eqs. (19), (20). This scenario is motivated by the fact we already discussed above [see the paragraph after Eqs. (31)] that our model correctly reproduces the charged lepton mass hierarchy with all the parameters $a_{11}^{(l)}, a_{12}^{(l)}, a_{21}^{(l)}, a_{22}^{(l)}$ of the order $\mathcal{O}(1)$. Setting all these parameters to be $a_{ij}^{(l)} = 1$ leads to a rather rough estimate of m_e and m_μ. Moreover, in this case $\tan\theta_l = 1$, which is incompatible with the neutrino oscillation data as seen from (35). Therefore, we release $a_{12}^{(l)}$ assuming it to be the only free parameter in the $e-\mu$-sector of charged leptons. Thus we consider a benchmark scenario (ii) with $a_{11}^{(l)} = a_{22}^{(l)} = a_{21}^{(l)} = 1$, $W_2 = W_3$. There are only four free parameters are W_1, W_2, κ and $a_{12}^{(l)}$ to reproduce seven observable: m_e, m_μ and five neutrino oscillation parameters. Note that the charged lepton $e-\mu$-sector depends only on one of these parameters, namely, $a_{12}^{(l)}$. It is tempting to try to make a prediction for m_μ starting from the best measured m_e. This also restricts the number of the free parameters in the neutrino sector down to W_1, W_2, κ. In this way we solve Eq. (19) with respect to $a_{12}^{(l)}$ for the central experimental value of m_e and predict m_μ using (20). The result is shown in Table 2 in the column (ii)' for $a_{12}^{(l)} = 0.52$ obtained from m_e. In the neutrino sector, having three parameters, the model is able to predict any two of the five observables using as an input the experimental values of the other three. However, as in the scenario (i) we fit all the neutrino oscillation observables, Δm^2_{21}, Δm^2_{31}, $\sin^2\theta_{12}$, $\sin^2\theta_{13}$, $\sin^2\theta_{23}$ with the model parameters W_1, W_2, κ. The best-fit values shown in the column (ii)' of Table 2 correspond to

$$\kappa = 0.71, \quad W_1 = 0.05\text{eV}^{\frac{1}{2}}, \quad W_2 = -0.17\text{eV}^{\frac{1}{2}}. \tag{36}$$

Now, instead of fixing $a_{12}^{(l)}$ from m_e, we fit all the model parameters $W_1, W_2, \kappa, a_{12}^{(l)}$ to seven observables m_e, m_μ and Δm^2_{21}, Δm^2_{31}, $\sin^2\theta_{12}$, $\sin^2\theta_{13}$, $\sin^2\theta_{23}$. The best-fit values are shown in the column (ii) of Table 2 and correspond to the following values of the model parameters:

$$\kappa \simeq 0.71, \quad W_1 \simeq 0.06\text{eV}^{\frac{1}{2}}, \\ W_2 \simeq -0.17\text{eV}^{\frac{1}{2}}, \quad a_{12}^{(l)} \simeq 0.56. \tag{37}$$

As seen from Table 3 in the scenario (ii) the neutrino oscillation parameters $\sin^2\theta_{12}$, $\sin^2\theta_{23}$, Δm^2_{21}, Δm^2_{31} are inside the 1σ experimentally allowed range. The reactor mixing parameter $\sin^2\theta_{13}$ is inside the 2σ range.

Now we evaluate in our model the effective Majorana neutrino mass parameter of neutrinoless double beta ($0\nu\beta\beta$) decay

$$m_{\beta\beta} = \left| \sum_j U_{ek}^2 m_{\nu_k} \right|, \tag{38}$$

where U_{ej}^2 and m_{ν_k} are the PMNS mixing matrix elements and the Majorana neutrino masses, respectively.

As we already mentioned the model parameters in Eq. (13) may have arbitrary complex phases. Therefore there may

Table 3 Range for experimental values of neutrino mass squared splittings and leptonic mixing parameters, taken from Ref. [113], for the case of normal hierarchy

Parameter	$\Delta m^2_{21}(10^{-5}\text{eV}^2)$	$\Delta m^2_{31}(10^{-3}\text{eV}^2)$	$\left(\sin^2\theta_{12}\right)_{\text{exp}}$	$\left(\sin^2\theta_{23}\right)_{\text{exp}}$	$\left(\sin^2\theta_{13}\right)_{\text{exp}}$
Best fit	7.60	2.48	0.323	0.567	0.0234
1σ range	7.42−7.79	2.41−2.53	0.307−0.339	0.439−0.599	0.0214−0.0254
2σ range	7.26−7.99	2.35−2.59	0.292−0.357	0.413−0.623	0.0195−0.0274
3σ range	7.11−8.11	2.30−2.65	0.278−0.375	0.392−0.643	0.0183−0.0297

occur cancellation between the terms in Eq. (38), which we are not able to control in the model. Thus we can predict only upper bounds for $m_{\beta\beta}$. For the parameters (32), (33) we find

$$m_{\beta\beta} \leq \begin{cases} 4 \text{ meV} & \text{for NH,} \\ 49 \text{ meV} & \text{for IH.} \end{cases} \tag{39}$$

Our obtained value $m_{\beta\beta} \approx 4$ meV for the effective Majorana neutrino mass parameter is beyond the reach of the present and forthcoming $0\nu\beta\beta$ decay experiments. The current best upper bound on the effective neutrino mass is $m_{\beta\beta} \leq 160$ meV, which corresponds to $T^{0\nu\beta\beta}_{1/2}(^{136}\text{Xe}) \geq 1.1 \times 10^{26}$ year at 90% C.L, as indicated by the KamLAND-Zen experiment [126]. This bound will be improved within a not too far future. The GERDA "phase-II"experiment [127,128] is expected to reach $T^{0\nu\beta\beta}_{1/2}(^{76}\text{Ge}) \geq 2 \times 10^{26}$ yr, which corresponds to $m_{\beta\beta} \leq 100$ meV. A bolometric CUORE experiment, using ^{130}Te [129], is currently under construction and has an estimated sensitivity of about $T^{0\nu\beta\beta}_{1/2}(^{130}\text{Te}) \sim 10^{26}$ year, which corresponds to $m_{\beta\beta} \leq 50$ meV. Furthermore, there are proposals for ton-scale next-to-next generation $0\nu\beta\beta$ experiments with ^{136}Xe [130,131] and ^{76}Ge [127,132], claiming sensitivities over $T^{0\nu\beta\beta}_{1/2} \sim 10^{27}$ yr, which corresponds to $m_{\beta\beta} \sim$12–30 meV. For a recent review, see for example Ref. [133]. Consequently, as follows from Eq. (39), our model predicts $T^{0\nu\beta\beta}_{1/2}$ at the level of sensitivities of the next generation or next-to-next generation $0\nu\beta\beta$ experiments.

5 Dark matter candidate

It is worth mentioning that there is a viable dark matter (DM) candidate in our model. If we consider a specific scenario where only the extra scalar doublet ϕ_2 acquires mass at low energy, while the rest of extra scalars and exotic fermions live at high energies, an approach to the well-known inert Higgs doublet model could be done. This model, originally proposed in [103] and extensively studied in a number of recent works [134,135], introduces an additional doublet, namely denoted in the literature as H_2, odd under an additional Z_2 symmetry. The lightest inert Z_2-odd particle turns out to be stable and hence a suitable DM candidate. Our additional scalar doublet ϕ_2, analogous to H_2, is odd under Z_2, which guarantees that it does not have direct couplings with SM fermion pairs and then its stability. The inert Higgs dark matter, in particular, could annihilate into WW^*, ZZ^*, hh^* and $t\bar{t}^*$. In the region restricted by the relic density constraint, i.e: $\Omega_{\text{DM}}h^2 = 0.1181 \pm 0.0012$ the annihilation on the DM into W^+W^- and ZZ is very effective, much more than annihilation into hh^* and $t\bar{t}^*$. The DM constraints can only be satisfied for restricted values of m_{ϕ_2}. In [135], three viable regions of DM are pointed out: a small regime with $3 \leq m_{H_2} \leq 50$ GeV, an intermediate regime with $60 \leq m_{H_2} \leq 100$ GeV and a large regime $3m_{H_2} \geq 550$ GeV. Therefore, if we expect ϕ_2 to be a DM candidate, its mass must fall in some of the three allowed regions. The limits on m_{ϕ_2} can be translated into some restrictions on the other model parameters, for example, ϵ^f_{ij} $(f = u, d, \nu)$, whose precise values are fixed by the requirement of having a realistic spectrum of SM fermion masses and mixing angles. The resulting constraints on the ϵ^l_{ij} parameters will yield bounds on the exotic fermion masses, thus setting limits on the total production cross sections of the non-SM particles at the LHC. Derivation of these constraints requires a dedicated study beyond the scope of the present paper and is left for future studies.

6 Conclusions

We have constructed an extension of the inert 2HDM, based on the extended $S_3 \otimes Z_2 \otimes Z_{12}$ symmetry that successfully describes the current pattern of SM fermion masses and mixings. In our model the Z_2 is preserved, whereas the S_3 and Z_{12} symmetries are broken, giving rise to the observed pattern of charged fermion masses and mixing angles. The preserved Z_2 symmetry allows the implementation of a one loop level radiative seesaw mechanism, which generates the masses for the first- and second-generation charged fermions, as well as a non-trivial quark mixing.

In our modified inert 2HDM, the SM fermion masses and mixing pattern arise from a combination of tree and one-loop-level effects. At tree level only the third-generation charged fermions acquire masses and there is no quark mixing, while the first- and second-generation charged fermion masses and the quark mixing arise from one loop level radiative seesaw-

type mechanisms, triggered by virtual Z_2-charged scalar fields and electrically charged exotic fermions running inside the loops. Light active neutrino masses are generated from a one-loop-level radiative seesaw mechanism.

As follows from the expressions for the loop functions given in Eq. (B2), the entries of the SM charged fermion and light active neutrino mass matrices generated at one-loop-level are monotonically decreasing functions of the masses of the other particles in the loops shown in Fig. 1. The condition that the mass matrices be compatible with the observed masses and mixing of the SM fermions sets constraints on the masses of the Z_2-odd scalars and the non-SM fermions. Derivation of these constraints requires a dedicated study because of the complexity of the model parameter space.

The preserved Z_2 symmetry of our model allows not only implementation of the radiative seesaw-type mechanism, but also provides natural dark matter candidates, stable due to this symmetry. They are the right-handed Majorana neutrinos N_{1R}, N_{2R} and/or the lightest of the Z_2 odd scalars Re η, Im η, Re ϕ_2^0, Im ϕ_2^0. Their masses are constrained by the dark matter relic density. The constraints on the masses of the Z_2 odd scalars states, will yield bounds on the total production cross sections of these particles at the LHC. The implications of our model in collider physics and dark matter requires careful studies that we left outside the scope of this paper and defer for a future publication.

Acknowledgements This work was partially supported by Fondecyt (Chile), Grants No. 1170803, No. 1150792, No. 1140390, No. 3150472 and by CONICYT (Chile) Ring ACT1406 and CONICYT PIA/Basal FB0821.

Appendices

Appendix A: The product rules of the S_3 discrete group

The S_3 group has three irreducible representations: $\mathbf{1}$, $\mathbf{1}'$ and $\mathbf{2}$. Denoting the basis vectors for two S_3 doublets as $(x_1, x_2)^T$ and $(y_1, y_2)^T$ and y' a non-trivial S_3 singlet, the multiplication rules for the S_3 discrete group take the form [1]:

$$\begin{pmatrix} x_1 \\ x_2 \end{pmatrix}_{\mathbf{2}} \otimes \begin{pmatrix} y_1 \\ y_2 \end{pmatrix}_{\mathbf{2}} = (x_1 y_1 + x_2 y_2)_{\mathbf{1}} + (x_1 y_2 - x_2 y_1)_{\mathbf{1}'} + \begin{pmatrix} x_2 y_2 - x_1 y_1 \\ x_1 y_2 + x_2 y_1 \end{pmatrix}_{\mathbf{2}}, \tag{A1}$$

$$\begin{pmatrix} x_1 \\ x_2 \end{pmatrix}_{\mathbf{2}} \otimes (y')_{\mathbf{1}'} = \begin{pmatrix} -x_2 y' \\ x_1 y' \end{pmatrix}_{\mathbf{2}}, \quad (x')_{\mathbf{1}'} \otimes (y')_{\mathbf{1}'} = (x' y')_{\mathbf{1}}. \tag{A2}$$

Appendix B: Analytical expressions for the dimensionless parameters of the SM fermion mass matrices generated at one loop level

The dimensionless parameters $\varepsilon_{ij}^{(u,d)}$ $(i, j = 1, 2, 3)$ generated at one loop level that appear in the SM quark mass matrices are given by

$$\begin{aligned}
\varepsilon_{11}^{(u)} &= \frac{1}{16\pi^2}\frac{C_{\phi_2\phi_1\eta} x_3^{(u)} y_1^{(u)}}{m_{T_1}} \times \left[C_0\left(\frac{m_{\mathrm{Re}\,\phi_2^0}}{m_{T_1}}, \frac{m_{\mathrm{Re}\,\eta}}{m_{T_1}}\right) - C_0\left(\frac{m_{\mathrm{Im}\,\phi_2^0}}{m_{T_1}}, \frac{m_{\mathrm{Im}\,\eta}}{m_{T_1}}\right)\right], \\
\varepsilon_{22}^{(u)} &= \frac{1}{16\pi^2}\frac{C_{\phi_2\phi_1\eta} x_4^{(u)} y_2^{(u)}}{m_{T_2}} \times \left[C_0\left(\frac{m_{\mathrm{Re}\,\phi_2^0}}{m_{T_2}}, \frac{m_{\mathrm{Re}\,\eta}}{m_{T_2}}\right) - C_0\left(\frac{m_{\mathrm{Im}\,\phi_2^0}}{m_{T_2}}, \frac{m_{\mathrm{Im}\,\eta}}{m_{T_2}}\right)\right], \\
\varepsilon_{13}^{(u)} &= \frac{1}{16\pi^2}\frac{C_{\phi_2\phi_1\eta} x_1^{(u)} y_1^{(u)}}{m_{T_1}} \times \left[C_0\left(\frac{m_{\mathrm{Re}\,\phi_2^0}}{m_{T_1}}, \frac{m_{\mathrm{Re}\,\eta}}{m_{T_1}}\right) - C_0\left(\frac{m_{\mathrm{Im}\,\phi_2^0}}{m_{T_1}}, \frac{m_{\mathrm{Im}\,\eta}}{m_{T_1}}\right)\right], \\
\varepsilon_{23}^{(u)} &= \frac{1}{16\pi^2}\frac{C_{\phi_2\phi_1\eta} x_2^{(u)} y_2^{(u)}}{m_{T_2}} \times \left[C_0\left(\frac{m_{\mathrm{Re}\,\phi_2^0}}{m_{T_2}}, \frac{m_{\mathrm{Re}\,\eta}}{m_{T_2}}\right) - C_0\left(\frac{m_{\mathrm{Im}\,\phi_2^0}}{m_{T_2}}, \frac{m_{\mathrm{Im}\,\eta}}{m_{T_2}}\right)\right], \\
\varepsilon_{11}^{(d)} &= \frac{1}{16\pi^2}\frac{C_{\phi_2\phi_1\eta} x_1^{(d)} y_1^{(d)}}{m_{B_1}} \times \left[C_0\left(\frac{m_{\mathrm{Re}\,\phi_2^0}}{m_{B_1}}, \frac{m_{\mathrm{Re}\,\eta}}{m_{B_1}}\right) - C_0\left(\frac{m_{\mathrm{Im}\,\phi_2^0}}{m_{B_1}}, \frac{m_{\mathrm{Im}\,\eta}}{m_{B_1}}\right)\right], \\
\varepsilon_{22}^{(d)} &= \frac{1}{16\pi^2}\frac{C_{\phi_2\phi_1\eta} x_4^{(d)} y_2^{(d)}}{m_{B_2}} \times \left[C_0\left(\frac{m_{\mathrm{Re}\,\phi_2^0}}{m_{B_2}}, \frac{m_{\mathrm{Re}\,\eta}}{m_{B_2}}\right) - C_0\left(\frac{m_{\mathrm{Im}\,\phi_2^0}}{m_{B_2}}, \frac{m_{\mathrm{Im}\,\eta}}{m_{B_2}}\right)\right], \\
\varepsilon_{21}^{(d)} &= \frac{1}{16\pi^2}\frac{C_{\phi_2\phi_1\eta} x_3^{(d)} y_2^{(d)}}{m_{B_2}} \times \left[C_0\left(\frac{m_{\mathrm{Re}\,\phi_2^0}}{m_{B_2}}, \frac{m_{\mathrm{Re}\,\eta}}{m_{B_2}}\right) - C_0\left(\frac{m_{\mathrm{Im}\,\phi_2^0}}{m_{B_2}}, \frac{m_{\mathrm{Im}\,\eta}}{m_{B_2}}\right)\right], \\
\varepsilon_{12}^{(d)} &= \frac{1}{16\pi^2}\frac{C_{\phi_2\phi_1\eta} x_2^{(d)} y_1^{(d)}}{m_{B_1}} \times \left[C_0\left(\frac{m_{\mathrm{Re}\,\phi_2^0}}{m_{B_1}}, \frac{m_{\mathrm{Re}\,\eta}}{m_{B_1}}\right) - C_0\left(\frac{m_{\mathrm{Im}\,\phi_2^0}}{m_{B_1}}, \frac{m_{\mathrm{Im}\,\eta}}{m_{B_1}}\right)\right],
\end{aligned} \tag{B1}$$

where the following function has been introduced:

$$C_0\left(\widehat{m}_1,\widehat{m}_2\right)=\frac{1}{\left(1-\widehat{m}_1^2\right)\left(1-\widehat{m}_2^2\right)\left(\widehat{m}_1^2-\widehat{m}_2^2\right)}\times\left\{\widehat{m}_1^2\widehat{m}_2^2\ln\left(\frac{\widehat{m}_1^2}{\widehat{m}_2^2}\right)-\widehat{m}_1^2\ln\widehat{m}_1^2+\widehat{m}_2^2\ln\widehat{m}_2^2\right\}. \tag{B2}$$

The dimensionless parameters $\varepsilon_{nm}^{(l)}$ $(n,m=1,2)$ generated at one loop level that appear in the SM charged lepton mass matrices take the form

$$\begin{aligned}
\varepsilon_{11}^{(l)} &= \frac{C_{\phi_2\phi_1\eta}}{16\pi^2}\left\{\frac{x_1^{(l)}y_1^{(l)}}{m_{E_1}}\left[C_0\left(\frac{m_{\mathrm{Re}\,\phi_2^0}}{m_{E_1}},\frac{m_{\mathrm{Re}\,\eta}}{m_{E_1}}\right)-C_0\left(\frac{m_{\mathrm{Im}\,\phi_2^0}}{m_{E_1}},\frac{m_{\mathrm{Im}\,\eta}}{m_{E_1}}\right)\right]\right.\\
&\left.+\frac{x_3^{(l)}y_3^{(l)}}{m_{E_2}}\left[C_0\left(\frac{m_{\mathrm{Re}\,\phi_2^0}}{m_{E_2}},\frac{m_{\mathrm{Re}\,\eta}}{m_{E_2}}\right)-C_0\left(\frac{m_{\mathrm{Im}\,\phi_2^0}}{m_{E_2}},\frac{m_{\mathrm{Im}\,\eta}}{m_{E_2}}\right)\right]\right\}\\
\varepsilon_{22}^{(l)} &= \frac{C_{\phi_2\phi_1\eta}}{16\pi^2}\left\{\frac{x_2^{(l)}y_2^{(l)}}{m_{E_1}}\left[C_0\left(\frac{m_{\mathrm{Re}\,\phi_2^0}}{m_{E_1}},\frac{m_{\mathrm{Re}\,\eta}}{m_{E_1}}\right)-C_0\left(\frac{m_{\mathrm{Im}\,\phi_2^0}}{m_{E_1}},\frac{m_{\mathrm{Im}\,\eta}}{m_{E_1}}\right)\right]\right.\\
&\left.+\frac{x_4^{(l)}y_4^{(l)}}{m_{E_2}}\left[C_0\left(\frac{m_{\mathrm{Re}\,\phi_2^0}}{m_{E_2}},\frac{m_{\mathrm{Re}\,\eta}}{m_{E_2}}\right)-C_0\left(\frac{m_{\mathrm{Im}\,\phi_2^0}}{m_{E_2}},\frac{m_{\mathrm{Im}\,\eta}}{m_{E_2}}\right)\right]\right\}\\
\varepsilon_{21}^{(l)} &= \frac{C_{\phi_2\phi_1\eta}}{16\pi^2}\left\{\frac{x_2^{(l)}y_1^{(l)}}{m_{E_1}}\left[C_0\left(\frac{m_{\mathrm{Re}\,\phi_2^0}}{m_{E_1}},\frac{m_{\mathrm{Re}\,\eta}}{m_{E_1}}\right)-C_0\left(\frac{m_{\mathrm{Im}\,\phi_2^0}}{m_{E_1}},\frac{m_{\mathrm{Im}\,\eta}}{m_{E_1}}\right)\right]\right.\\
&\left.+\frac{x_4^{(l)}y_3^{(l)}}{m_{E_2}}\left[C_0\left(\frac{m_{\mathrm{Re}\,\phi_2^0}}{m_{E_2}},\frac{m_{\mathrm{Re}\,\eta}}{m_{E_2}}\right)-C_0\left(\frac{m_{\mathrm{Im}\,\phi_2^0}}{m_{E_2}},\frac{m_{\mathrm{Im}\,\eta}}{m_{E_2}}\right)\right]\right\}\\
\varepsilon_{12}^{(l)} &= \frac{C_{\phi_2\phi_1\eta}}{16\pi^2}\left\{\frac{x_1^{(l)}y_2^{(l)}}{m_{E_1}}\left[C_0\left(\frac{m_{\mathrm{Re}\,\phi_2^0}}{m_{E_1}},\frac{m_{\mathrm{Re}\,\eta}}{m_{E_1}}\right)-C_0\left(\frac{m_{\mathrm{Im}\,\phi_2^0}}{m_{E_1}},\frac{m_{\mathrm{Im}\,\eta}}{m_{E_1}}\right)\right]\right.\\
&\left.+\frac{x_3^{(l)}y_4^{(l)}}{m_{E_2}}\left[C_0\left(\frac{m_{\mathrm{Re}\,\phi_2^0}}{m_{E_2}},\frac{m_{\mathrm{Re}\,\eta}}{m_{E_2}}\right)-C_0\left(\frac{m_{\mathrm{Im}\,\phi_2^0}}{m_{E_2}},\frac{m_{\mathrm{Im}\,\eta}}{m_{E_2}}\right)\right]\right\}.
\end{aligned} \tag{B3}$$

References

1. H. Ishimori, T. Kobayashi, H. Ohki, Y. Shimizu, H. Okada, M. Tanimoto, Prog. Theor. Phys. Suppl. **183**, 1 (2010). doi:10.1143/PTPS.183.1. arXiv:1003.3552 [hep-th]
2. G. Altarelli, F. Feruglio, Rev. Mod. Phys. **82**, 2701 (2010). doi:10.1103/RevModPhys.82.2701. arXiv:1002.0211 [hep-ph]
3. S.F. King, C. Luhn, Rep. Prog. Phys. **76**, 056201 (2013). doi:10.1088/0034-4885/76/5/056201. arXiv:1301.1340 [hep-ph]
4. S.F. King, A. Merle, S. Morisi, Y. Shimizu, M. Tanimoto, New J. Phys. **16**, 045018 (2014). doi:10.1088/1367-2630/16/4/045018. arXiv:1402.4271 [hep-ph]
5. S. Pakvasa, H. Sugawara, Phys. Lett. **73B**, 61 (1978). doi:10.1016/0370-2693(78)90172-7
6. H. Cardenas, A.C.B. Machado, V. Pleitez, J.-A. Rodriguez, Phys. Rev. D **87**(3), 035028 (2013). doi:10.1103/PhysRevD.87.035028. arXiv:1212.1665 [hep-ph]
7. A.G. Dias, A.C.B. Machado, C.C. Nishi, Phys. Rev. D **86**, 093005 (2012). doi:10.1103/PhysRevD.86.093005. arXiv:1206.6362 [hep-ph]
8. S. Dev, R.R. Gautam, L. Singh, Phys. Lett. B **708**, 284 (2012). doi:10.1016/j.physletb.2012.01.051. arXiv:1201.3755 [hep-ph]
9. D. Meloni, JHEP **1205**, 124 (2012). doi:10.1007/JHEP05(2012)124. arXiv:1203.3126 [hep-ph]
10. F. González Canales, A. Mondragón, M. Mondragón, U.J. Saldaña Salazar, L. Velasco-Sevilla. Phys. Rev. D **88**, 096004 (2013). doi:10.1103/PhysRevD.88.096004. arXiv:1304.6644 [hep-ph]
11. E. Ma, B. Melic, Phys. Lett. B **725**, 402 (2013). doi:10.1016/j.physletb.2013.07.015. arXiv:1303.6928 [hep-ph]
12. Y. Kajiyama, H. Okada, K. Yagyu, Nucl. Phys. B **887**, 358 (2014). doi:10.1016/j.nuclphysb.2014.08.009. arXiv:1309.6234 [hep-ph]
13. A.E. Cárcamo Hernández, R. Martinez, F. Ochoa, Eur. Phys. J. C **76**(11), 634 (2016). doi:10.1140/epjc/s10052-016-4480-3. arXiv:1309.6567 [hep-ph]
14. A.E. Cárcamo Hernández, E. Cataño Mur, R. Martinez, Phys. Rev. D **90**(7), 073001 (2014). doi:10.1103/PhysRevD.90.073001. arXiv:1407.5217 [hep-ph]
15. A.E. Cárcamo Hernández, R. Martinez, J. Nisperuza, Eur. Phys. J. C **75**(2), 72 (2015). doi:10.1140/epjc/s10052-015-3278-z. arXiv:1401.0937 [hep-ph]
16. V.V. Vien, H.N. Long, Zh Eksp, Teor. Fiz. **145**, 991 (2014)
17. V.V. Vien, H.N. Long, J. Exp. Theor. Phys. **118**(6), 869 (2014). doi:10.7868/S0044451014060044. doi:10.1134/S1063776114050173. arXiv:1404.6119 [hep-ph]
18. E. Ma, R. Srivastava, Phys. Lett. B **741**, 217 (2015). doi:10.1016/j.physletb.2014.12.049. arXiv:1411.5042 [hep-ph]
19. D. Das, U.K. Dey, P.B. Pal, Phys. Lett. B **753**, 315 (2016). doi:10.1016/j.physletb.2015.12.038. arXiv:1507.06509 [hep-ph]
20. A.E. Cárcamo Hernández, I. de Medeiros Varzielas, E. Schumacher, Phys. Rev. D **93**(1), 016003 (2016). doi:10.1103/PhysRevD.93.016003. arXiv:1509.02083 [hep-ph]
21. A.E. Cárcamo Hernández, I. de Medeiros Varzielas, N.A. Neill, Phys. Rev. D **94**(3), 033011 (2016). doi:10.1103/PhysRevD.94.033011. arXiv:1511.07420 [hep-ph]
22. A.E. Cárcamo Hernández, I. de Medeiros Varzielas, E. Schumacher, arXiv:1601.00661 [hep-ph]
23. A.E. Cárcamo Hernández, Eur. Phys. J. C **76**(9), 503 (2016). doi:10.1140/epjc/s10052-016-4351-y. arXiv:1512.09092 [hep-ph]
24. A.E. Cárcamo Hernández, S. Kovalenko, I. Schmidt, JHEP **1702**, 125 (2017). doi:10.1007/JHEP02(2017)125. arXiv:1611.09797 [hep-ph]
25. Z.Z. Xing, D. Yang, S. Zhou, Phys. Lett. B **690**, 304 (2010). doi:10.1016/j.physletb.2010.05.045. arXiv:1004.4234 [hep-ph]
26. E. Ma, G. Rajasekaran, Phys. Rev. D **64**, 113012 (2001). doi:10.1103/PhysRevD.64.113012. arXiv:hep-ph/0106291
27. K.S. Babu, E. Ma, J.W.F. Valle, Phys. Lett. B **552**, 207 (2003). doi:10.1016/S0370-2693(02)03153-2. arXiv:hep-ph/0206292
28. G. Altarelli, F. Feruglio, Nucl. Phys. B **720**, 64 (2005). doi:10.1016/j.nuclphysb.2005.05.005. arXiv:hep-ph/0504165
29. G. Altarelli, F. Feruglio, Nucl. Phys. B **741**, 215 (2006). doi:10.1016/j.nuclphysb.2006.02.015. arXiv:hep-ph/0512103
30. I. de Medeiros Varzielas, S.F. King, G.G. Ross, Phys. Lett. B **644**, 153 (2007). doi:10.1016/j.physletb.2006.11.015. arXiv:hep-ph/0512313
31. X.G. He, Y.Y. Keum, R.R. Volkas, JHEP **0604**, 039 (2006). doi:10.1088/1126-6708/2006/04/039. arXiv:hep-ph/0601001
32. I. de Medeiros Varzielas, D. Pidt, JHEP **1303**, 065 (2013). doi:10.1007/JHEP03(2013)065. arXiv:1211.5370 [hep-ph]
33. I.K. Cooper, S.F. King, C. Luhn, JHEP **1206**, 130 (2012). doi:10.1007/JHEP06(2012)130. arXiv:1203.1324 [hep-ph]
34. H. Ishimori, E. Ma, Phys. Rev. D **86**, 045030 (2012). doi:10.1103/PhysRevD.86.045030. arXiv:1205.0075 [hep-ph]
35. Y.H. Ahn, S.K. Kang, C.S. Kim, Phys. Rev. D **87**(11), 113012 (2013). doi:10.1103/PhysRevD.87.113012. arXiv:1304.0921 [hep-ph]
36. N. Memenga, W. Rodejohann, H. Zhang, Phys. Rev. D **87**(5), 053021 (2013). doi:10.1103/PhysRevD.87.053021. arXiv:1301.2963 [hep-ph]

37. S. Bhattacharya, E. Ma, A. Natale, A. Rashed, Phys. Rev. D **87**, 097301 (2013). doi:10.1103/PhysRevD.87.097301. arXiv:1302.6266 [hep-ph]
38. P.M. Ferreira, L. Lavoura, P.O. Ludl, Phys. Lett. B **726**, 767 (2013). doi:10.1016/j.physletb.2013.09.058. arXiv:1306.1500 [hep-ph]
39. R. Gonzalez Felipe, H. Serodio, J.P. Silva, Phys. Rev. D **88**(1), 015015 (2013). doi:10.1103/PhysRevD.88.015015. arXiv:1304.3468 [hep-ph]
40. A.E. Carcamo Hernandez, I. de Medeiros Varzielas, S.G. Kovalenko, H. Päs, I. Schmidt, Phys. Rev. D **88**(7), 076014 (2013). doi:10.1103/PhysRevD.88.076014. arXiv:1307.6499 [hep-ph]
41. S.F. King, S. Morisi, E. Peinado, J.W.F. Valle, Phys. Lett. B **724**, 68 (2013). doi:10.1016/j.physletb.2013.05.067. arXiv:1301.7065 [hep-ph]
42. S. Morisi, D.V. Forero, J.C. Romão, J.W.F. Valle, Phys. Rev. D **88**(1), 016003 (2013). doi:10.1103/PhysRevD.88.016003. arXiv:1305.6774 [hep-ph]
43. S. Morisi, M. Nebot, K.M. Patel, E. Peinado, J.W.F. Valle, Phys. Rev. D **88**, 036001 (2013). doi:10.1103/PhysRevD.88.036001. arXiv:1303.4394 [hep-ph]
44. R. González Felipe, H. Serôdio, J.P. Silva, Phys. Rev. D **87**(5), 055010 (2013). doi:10.1103/PhysRevD.87.055010. arXiv:1302.0861 [hep-ph]
45. S.F. King, JHEP **1408**, 130 (2014). doi:10.1007/JHEP08(2014)130. arXiv:1406.7005 [hep-ph]
46. B. Karmakar, A. Sil, Phys. Rev. D **91**, 013004 (2015). doi:10.1103/PhysRevD.91.013004. arXiv:1407.5826 [hep-ph]
47. M.D. Campos, A.E. Cárcamo Hernández, S. Kovalenko, I. Schmidt, E. Schumacher, Phys. Rev. D **90**(1), 016006 (2014). doi:10.1103/PhysRevD.90.016006. arXiv:1403.2525 [hep-ph]
48. A.E. Cárcamo Hernández, R. Martinez. Nucl. Phys. B **905**, 337 (2016). doi:10.1016/j.nuclphysb.2016.02.025. arXiv:1501.05937 [hep-ph]
49. B. Karmakar, A. Sil, Phys. Rev. D **93**(1), 013006 (2016). doi:10.1103/PhysRevD.93.013006. arXiv:1509.07090 [hep-ph]
50. S. Pramanick, A. Raychaudhuri, Phys. Rev. D **93**(3), 033007 (2016). doi:10.1103/PhysRevD.93.033007. arXiv:1508.02330 [hep-ph]
51. C. Bonilla, M. Nebot, R. Srivastava, J.W.F. Valle, Phys. Rev. D **93**(7), 073009 (2016). doi:10.1103/PhysRevD.93.073009. arXiv:1602.08092 [hep-ph]
52. A.S. Belyaev, J.E. Camargo-Molina, S.F. King, D.J. Miller, A.P. Morais, P.B. Schaefers, JHEP **1606**, 142 (2016). doi:10.1007/JHEP06(2016)142. arXiv:1605.02072 [hep-ph]
53. A.E. Cárcamo Hernández, S. Kovalenko, H.N. Long, I. Schmidt, arXiv:1705.09169 [hep-ph]
54. A.E. Cárcamo Hernández, H.N. Long, arXiv:1705.05246 [hep-ph]
55. R.Z. Yang, H. Zhang, Phys. Lett. B **700**, 316 (2011). doi:10.1016/j.physletb.2011.05.014. arXiv:1104.0380 [hep-ph]
56. P.S. Bhupal Dev, B. Dutta, R.N. Mohapatra, M. Severson, Phys. Rev. D **86**, 035002 (2012). doi:10.1103/PhysRevD.86.035002. arXiv:1202.4012 [hep-ph]
57. R.N. Mohapatra, C.C. Nishi, Phys. Rev. D **86**, 073007 (2012). doi:10.1103/PhysRevD.86.073007. arXiv:1208.2875 [hep-ph]
58. I. de Medeiros Varzielas, L. Lavoura, J. Phys. G **40**, 085002 (2013). doi:10.1088/0954-3899/40/8/085002. arXiv:1212.3247 [hep-ph]
59. G.J. Ding, S.F. King, C. Luhn, A.J. Stuart, JHEP **1305**, 084 (2013). doi:10.1007/JHEP05(2013)084. arXiv:1303.6180 [hep-ph]
60. H. Ishimori, Y. Shimizu, M. Tanimoto, A. Watanabe, Phys. Rev. D **83**, 033004 (2011). doi:10.1103/PhysRevD.83.033004. arXiv:1010.3805 [hep-ph]
61. G.J. Ding, Y.L. Zhou, Nucl. Phys. B **876**, 418 (2013). doi:10.1016/j.nuclphysb.2013.08.011. arXiv:1304.2645 [hep-ph]
62. C. Hagedorn, M. Serone, JHEP **1110**, 083 (2011). doi:10.1007/JHEP10(2011)083. arXiv:1106.4021 [hep-ph]
63. M.D. Campos, A.E. Cárcamo Hernández, H. Päs, E. Schumacher, Phys. Rev. D **91**(11), 116011 (2015). doi:10.1103/PhysRevD.91.116011. arXiv:1408.1652 [hep-ph]
64. C. Luhn, S. Nasri, P. Ramond, Phys. Lett. B **652**, 27 (2007). doi:10.1016/j.physletb.2007.06.059. arXiv:0706.2341 [hep-ph]
65. C. Hagedorn, M.A. Schmidt, A.Y. Smirnov, Phys. Rev. D **79**, 036002 (2009). doi:10.1103/PhysRevD.79.036002. arXiv:0811.2955 [hep-ph]
66. Q.H. Cao, S. Khalil, E. Ma, H. Okada, Phys. Rev. Lett. **106**, 131801 (2011). doi:10.1103/PhysRevLett.106.131801. arXiv:1009.5415 [hep-ph]
67. C. Luhn, K.M. Parattu, A. Wingerter, JHEP **1212**, 096 (2012). doi:10.1007/JHEP12(2012)096. arXiv:1210.1197 [hep-ph]
68. Y. Kajiyama, H. Okada, K. Yagyu, JHEP **1310**, 196 (2013). doi:10.1007/JHEP10(2013)196. arXiv:1307.0480 [hep-ph]
69. C. Bonilla, S. Morisi, E. Peinado, J.W.F. Valle, Phys. Lett. B **742**, 99 (2015). doi:10.1016/j.physletb.2015.01.017. arXiv:1411.4883 [hep-ph]
70. A.E. Cárcamo Hernández, R. Martinez, J. Phys. G **43**(4), 045003 (2016). doi:10.1088/0954-3899/43/4/045003. arXiv:1501.07261 [hep-ph]
71. C. Arbeláez, A.E. Cárcamo Hernández, S. Kovalenko, I. Schmidt, Phys. Rev. D **92**(11), 115015 (2015). doi:10.1103/PhysRevD.92.115015. arXiv:1507.03852 [hep-ph]
72. A.E. Cárcamo Hernández, R. Martinez, PoS PLANCK **2015**, 023 (2015). arXiv:1511.07997 [hep-ph]
73. I. de Medeiros Varzielas, S.F. King, G.G. Ross, Phys. Lett. B **648**, 201 (2007). doi:10.1016/j.physletb.2007.03.009. arXiv:hep-ph/0607045
74. E. Ma, Mod. Phys. Lett. A **21**, 1917 (2006). doi:10.1142/S0217732306021190. arXiv:hep-ph/0607056
75. I. de Medeiros Varzielas, D. Emmanuel-Costa, P. Leser, Phys. Lett. B **716**, 193 (2012). doi:10.1016/j.physletb.2012.08.008. arXiv:1204.3633 [hep-ph]
76. G. Bhattacharyya, I. de Medeiros, Varzielas and P. Leser. Phys. Rev. Lett. **109**, 241603 (2012). doi:10.1103/PhysRevLett.109.241603. arXiv:1210.0545 [hep-ph]
77. P.M. Ferreira, W. Grimus, L. Lavoura, P.O. Ludl, JHEP **1209**, 128 (2012). doi:10.1007/JHEP09(2012)128. arXiv:1206.7072 [hep-ph]
78. E. Ma, Phys. Lett. B **723**, 161 (2013). doi:10.1016/j.physletb.2013.05.011. arXiv:1304.1603 [hep-ph]
79. C.C. Nishi, Phys. Rev. D **88**(3), 033010 (2013). doi:10.1103/PhysRevD.88.033010. arXiv:1306.0877 [hep-ph]
80. I. de Medeiros Varzielas, D. Pidt, J. Phys. G **41**, 025004 (2014). doi:10.1088/0954-3899/41/2/025004. arXiv:1307.0711 [hep-ph]
81. A. Aranda, C. Bonilla, S. Morisi, E. Peinado, J.W.F. Valle, Phys. Rev. D **89**(3), 033001 (2014). doi:10.1103/PhysRevD.89.033001. arXiv:1307.3553 [hep-ph]
82. I. de Medeiros Varzielas, D. Pidt, JHEP **1311**, 206 (2013). doi:10.1007/JHEP11(2013)206. arXiv:1307.6545 [hep-ph]
83. M. Abbas, S. Khalil, Phys. Rev. D **91**(5), 053003 (2015). doi:10.1103/PhysRevD.91.053003. arXiv:1406.6716 [hep-ph]
84. I. de Medeiros Varzielas, JHEP **1508**, 157 (2015). doi:10.1007/JHEP08(2015)157. arXiv:1507.00338 [hep-ph]
85. F. Björkeroth, F.J. de Anda, I. de Medeiros Varzielas, S.F. King, Phys. Rev. D **94**(1), 016006 (2016). doi:10.1103/PhysRevD.94.016006. arXiv:1512.00850 [hep-ph]
86. P. Chen, G.J. Ding, A.D. Rojas, C.A. Vaquera-Araujo, J.W.F. Valle, JHEP **1601**, 007 (2016). doi:10.1007/JHEP01(2016)007. arXiv:1509.06683 [hep-ph]

87. M. Abbas, S. Khalil, A. Rashed, A. Sil, Phys. Rev. D **93**(1), 013018 (2016). doi:10.1103/PhysRevD.93.013018. arXiv:1508.03727 [hep-ph]
88. V.V. Vien, A.E. Cárcamo Hernández, H.N. Long. Nucl. Phys. B **913**, 792 (2016). doi:10.1016/j.nuclphysb.2016.10.010. arXiv:1601.03300 [hep-ph]
89. A.E. Cárcamo Hernández, H.N. Long, V.V. Vien, Eur. Phys. J. C **76**(5), 242 (2016). doi:10.1140/epjc/s10052-016-4074-0. arXiv:1601.05062 [hep-ph]
90. S.C. Chuliá, R. Srivastava, J.W.F. Valle, Phys. Lett. B **761**, 431 (2016). doi:10.1016/j.physletb.2016.08.028. arXiv:1606.06904 [hep-ph]
91. A.E. Cárcamo Hernández, S. Kovalenko, J.W.F. Valle, C.A. Vaquera-Araujo, arXiv:1705.06320 [hep-ph]
92. E. Ma, D. Ng, J.T. Pantaleone, G.G. Wong, Phys. Rev. D **40**, 1586 (1989). doi:10.1103/PhysRevD.40.1586
93. E. Ma, D. Ng, G.G. Wong, Z. Phys. C **47**, 431 (1990). doi:10.1007/BF01565864
94. P.V. Dong, D.T. Huong, T.T. Huong, H.N. Long, Phys. Rev. D **74**, 053003 (2006). doi:10.1103/PhysRevD.74.053003. arXiv:hep-ph/0607291
95. A.E. Carcamo Hernandez, R. Martinez, F. Ochoa, Phys. Rev. D **87**(7), 075009 (2013). doi:10.1103/PhysRevD.87.075009. arXiv:1302.1757 [hep-ph]
96. R. Adhikari, D. Borah, E. Ma, Phys. Lett. B **755**, 414 (2016). doi:10.1016/j.physletb.2016.02.039. arXiv:1512.05491 [hep-ph]
97. T. Nomura, H. Okada, Phys. Lett. B **761**, 190 (2016). doi:10.1016/j.physletb.2016.08.023. arXiv:1606.09055 [hep-ph]
98. C. Kownacki, E. Ma, Phys. Lett. B **760**, 59 (2016). doi:10.1016/j.physletb.2016.06.024. arXiv:1604.01148 [hep-ph]
99. T. Nomura, H. Okada, N. Okada, Phys. Lett. B **762**, 409 (2016). doi:10.1016/j.physletb.2016.09.038. arXiv:1608.02694 [hep-ph]
100. R. Gatto, G. Sartori, M. Tonin, Phys. Lett. **28B**, 128 (1968). doi:10.1016/0370-2693(68)90150-0
101. N. Cabibbo, L. Maiani, Phys. Lett. **28B**, 131 (1968). doi:10.1016/0370-2693(68)90151-2
102. R.J. Oakes, Phys. Lett. **29B**, 683 (1969). doi:10.1016/0370-2693(69)90110-5
103. N.G. Deshpande, E. Ma, Phys. Rev. D **18**, 2574 (1978). doi:10.1103/PhysRevD.18.2574
104. G.C. Branco, D. Emmanuel-Costa, C. Simoes, Phys. Lett. B **690**, 62 (2010). doi:10.1016/j.physletb.2010.05.009. arXiv:1001.5065 [hep-ph]
105. H. Ishimori, S.F. King, Phys. Lett. B **735**, 33 (2014). doi:10.1016/j.physletb.2014.06.003. arXiv:1403.4395 [hep-ph]
106. H. Ishimori, S.F. King, H. Okada, M. Tanimoto, Phys. Lett. B **743**, 172 (2015). doi:10.1016/j.physletb.2015.02.027. arXiv:1411.5845 [hep-ph]
107. A.E. Carcamo Hernandez, C.O. Dib, N. Neill, A.R. Zerwekh, JHEP **1202**, 132 (2012). doi:10.1007/JHEP02(2012)132. arXiv:1201.0878 [hep-ph]
108. V.V. Vien, H.N. Long, J. Korean Phys. Soc. **66**(12), 1809 (2015). doi:10.3938/jkps.66.1809. arXiv:1408.4333 [hep-ph]
109. G.C. Branco, H.R.C. Ferreira, A.G. Hessler, J.I. Silva-Marcos, JHEP **1205**, 001 (2012). doi:10.1007/JHEP05(2012)001. arXiv:1101.5808 [hep-ph]
110. C. Patrignani et al. [Particle Data Group], Chin. Phys. C **40**(10), 100001 (2016). doi:10.1088/1674-1137/40/10/100001
111. K. Bora, Horizon **2** (2013). arXiv:1206.5909 [hep-ph]
112. Z.Z. Xing, H. Zhang, S. Zhou, Phys. Rev. D **77**, 113016 (2008). doi:10.1103/PhysRevD.77.113016. arXiv:0712.1419 [hep-ph]
113. D.V. Forero, M. Tortola, J.W.F. Valle, Phys. Rev. D **90**(9), 093006 (2014). doi:10.1103/PhysRevD.90.093006. arXiv:1405.7540 [hep-ph]
114. T. Fukuyama, H. Nishiura, arXiv:hep-ph/9702253
115. C.S. Lam, Phys. Lett. B **507**, 214 (2001)
116. W. Grimus, L. Lavoura, JHEP **0107**, 045 (2001)
117. W. Grimus, L. Lavoura, Eur. Phys. J. C **28**, 123 (2003)
118. T. Kitabayashi, M. Yasue, Phys. Rev. D **67**, 015006 (2003)
119. Y. Koide, Phys. Rev. D **69**, 093001 (2004)
120. P.F. Harrison, W.G. Scott, Phys. Lett. B **547**, 219 (2002)
121. W. Grimus, A.S. Joshipura, S. Kaneko, L. Lavoura, H. Sawanaka, M. Tanimoto, Nucl. Phys. B **713**, 151 (2005)
122. S. Choubey, W. Rodejohann, Eur. Phys. J. C **40**, 259 (2005)
123. R.N. Mohapatra, S. Nasri, H.B. Yu, Phys. Lett. B **615**, 231 (2005)
124. C.S. Lam, Phys. Rev. D **71**, 093001 (2005)
125. R.N. Mohapatra, JHEP **0410**, 027 (2004)
126. A. Gando et al. [KamLAND-Zen Collaboration], Phys. Rev. Lett. **117**(8), 082503 (2016). Addendum: [Phys. Rev. Lett. **117**(10), 109903 (2016)]. doi:10.1103/PhysRevLett.117.109903. doi:10.1103/PhysRevLett.117.082503. arXiv:1605.02889 [hep-ex]
127. I. Abt et al., arXiv:hep-ex/0404039
128. K.H. Ackermann et al. [GERDA Collaboration], Eur. Phys. J. C **73**(3), 2330 (2013). doi:10.1140/epjc/s10052-013-2330-0. arXiv:1212.4067 [physics.ins-det]
129. F. Alessandria et al., arXiv:1109.0494 [nucl-ex]
130. A. Gando et al. [KamLAND-Zen Collaboration], Phys. Rev. C **85**, 045504 (2012). doi:10.1103/PhysRevC.85.045504. arXiv:1201.4664 [hep-ex]
131. J.B. Albert et al. [EXO-200 Collaboration], Phys. Rev. D **90**(9), 092004 (2014). doi:10.1103/PhysRevD.90.092004. arXiv:1409.6829 [hep-ex]
132. C.E. Aalseth et al. [Majorana Collaboration], Nucl. Phys. Proc. Suppl. **217**, 44 (2011). doi:10.1016/j.nuclphysbps.2011.04.063. arXiv:1101.0119 [nucl-ex]
133. S.M. Bilenky, C. Giunti, Int. J. Mod. Phys. A **30**(04n05), 1530001 (2015). doi:10.1142/S0217751X1530001X. arXiv:1411.4791 [hep-ph]
134. L. Lopez Honorez, C.E. Yaguna, JHEP **1009**, 046 (2010). doi:10.1007/JHEP09(2010)046. arXiv:1003.3125 [hep-ph]
135. M.A. Díaz, B. Koch, S. Urrutia-Quiroga, Adv. High Energy Phys. **2016**, 8278375 (2016). doi:10.1155/2016/8278375. arXiv:1511.04429 [hep-ph]